NETL
NATIONAL ENERGY TECHNOLOGY LABORATORY

Extent of Hydraulic Fractures in Shales

9 December 2016

Disclaimer

Cover Illustration: A schematic diagram of a hydraulic fracture.

An electronic version of this report can be found at:
http://www.netl.doe.gov/research/on-site-research/publications/featured-technical-reports

https://edx.netl.doe.gov/ucr

Extent of Hydraulic Fractures in Shales

Hema Siriwardane[1,2], Raj Gondle[1,2], Grant Bromhal[1]

[1]U.S. Department of Energy, National Energy Technology Laboratory, 3610 Collins Ferry Road, Morgantown, WV 26507

[2]Department of Civil and Environmental Engineering, West Virginia University, Morgantown, WV 26506

This page intentionally left blank.

Table of Contents

This page intentionally left blank.

List of Figures

List of Tables

Acronyms, Abbreviations, and Symbols

Term	Description
2-D	Two-dimensional
τ	Fluid loss delay time
τ_f	Friction coefficient
ΔP	Pressure differential, $(P_f - S_1)$
η	Fracture efficiency
υ	Poisson's ratio
ac	acres
bpm	Barrels per minute
C_{leak}	Total leak-off coefficient
d_f	Depth of fracture
d_i	Injection depth
G	Shear Modulus
GDK	Geertsma-De-Klerk model
H	Fracture half height
Hp	Pay zone height
H_w	Total fracture height at the wellbore
Ka	Apparent consistency index
L	Fracture half length
MCF	Million cubic feet
n'	Slurry flow behavior index
P	Pressure
PKN	Perkins and Kern model
Q	Total flow rate
r	Radial coordinate
R	Fracture radius
s	Dimensionless vertical coordinate, s = z / H
s'	Dimensionless lateral coordinate, s' = x / L
SCF	Standard cubic foot
t	Time
TCF	Trillion cubic foot

Acronyms, Abbreviations, Symbols (cont.)

Term	Description
W	Width of fracture
W_w	Maximum fracture width at the wellbore
x	Lateral coordinate along fracture length
z	Vertical coordinate

Acknowledgments

This page intentionally left blank.

EXECUTIVE SUMMARY

The purpose of this work was to determine the extent of the potential damage zone in geologic formations above the pay zone during stimulation of gas shale reservoirs. Four different shale formations were considered in this study: Barnett shale, Marcellus shale, Fayetteville shale, and Haynesville shale. In this study, the fracture length, fracture height, and fracture width were determined for different volumes of fluid injection in different types of shale reservoirs. The computations were based on three existing theories of fracture propagation: the Perkins and Kern model (PKN) (Perkins and Kern, 1961; Nordgren, 1972), Geertsma-De-Klerk model (GDK) (Geertsma and De Klerk, 1969), and the Ellipsoidal model (Meyer & Associates, 2009). According to these models the hydraulic fracture lies along a single plane. The study was based on the assumption of a penny-shaped, a constant-height, or an ellipsoidal-shaped fracture that is generated at the center of the shale layer during hydraulic fracturing. The results from these models were used to assess dependency of the predictions on the underlying theory. The computations were performed on the basis of assumed rock properties.

In the present study, the objective was to determine whether hydraulic fractures would propagate beyond the pay zone and, if so, how far. As such, the emphasis in this study was the fracture height. The fracture length, fracture height, and fracture width were determined for different volumes of fluid injection in different shale formations. The computer code MFAST (Meyer & Associates, 2009) is capable of predicting how hydraulically-induced fractures propagate in subsurface formations by using different fracture propagation theories. This code was used in this study because of its capability to include simplified assumptions on fracture geometry. In these simulations, the vertical extent of the fracture was not restricted to the reservoir thickness. Instead, the fractures were allowed to propagate in the vertical direction without any constraints. It was assumed that the vertical fracture propagation occurs towards the ground surface rather than propagating below the pay zone. Results show an increase in the fracture length and fracture height with an increase in the injection volume and injection rate. The clearance depth to groundwater table was investigated for fracture propagation in Barnett, Marcellus, Fayetteville, and Haynesville shale reservoirs. The depth of injection was assumed to be at the middle of the payzone layer. The depth to fracture was calculated.

The Haynesville shale is the deepest shale layer considered in this study. The depth to the top of fracture (clearance depth) is the largest for the Haynesville shale in comparison to other shale formations (Marcellus, Fayetteville, and Barnett). Results also show that Fayetteville shale formations have the lowest clearance depth among the four shale basins considered in this study. Results show that the computed value of fracture height is the largest for the Barnett shale at a fluid injection rate of 120 barrels per minute (bpm).

Of the three models considered, the Ellipsoidal fracture model predicts the largest fracture height in general. The uncertainties of these predictions include the uncertainties of material properties used. The models did not include any consideration of natural fractures that may be present in the rock formations. The clearance depth computed in this study is within the range of values reported in the literature (Fisher and Warpinski, 2011) for Barnett and Marcellus shales, but no field data has been reported for Haynesville and Fayetteville shales in the this reference. Computed clearance depth for the Barnett, Marcellus, and Haynesville shales is well over 4,300 ft from the ground surface. For Fayettville shale, the calculated clearance depth is 1,505 ft for the

assumed injection volumes and rates. The clearance depth can be increased by reducing the injection volumes and injection rates.

1. <u>INTRODUCTION</u>

1.1 BACKGROUND

Hydraulic fracturing is a fracture stimulation process used in tight geologic formations such as gas shales. Large amounts of water, sand, and other substances are pumped underground to initiate and propagate fractures to enhance natural gas recovery as shown in Figure 1.

During this process, fractures may propagate beyond the pay zone. Public debate over hydraulic fracturing has included a concern for the potential of fractures to extend so far out of zone that they could propagate to groundwater resources thousands of feet above the reservoir. Industry data, however, documents a limited extent of fracturing out of zone, as observed by microseismicity (Fisher and Warpinski, 2011); these data suggest fracture propagation out of zone may vary with depth (and perhaps lithology), but the fractures remain thousands of feet below groundwater resources for the shales studied.

In order to provide confidence in the understanding of fracture propagation out of zone, this study used the established fracture growth models based on very simple assumptions, combined with site-relevant data on rock properties to assess the likely maximum extent of fracture propagation out of zone.

The objective of this study is to determine whether hydraulic fractures would propagate beyond the pay zone and, if so, how far. Four major gas shale formations (Barnett, Marcellus, Fayetteville, and Haynesville) were assessed in the study. Figure 2 shows the locations of these basins. Data on reservoir properties needed for the simulations—such as gas content, gas-in-place, reservoir depth, and depth of the base of groundwater table in these formations—were based on a detailed evaluation of published scientific literature. Table 1 shows a list of properties for the four major gas shale basins (Barnett, Marcellus, Haynesville, and Fayetteville) in the United States (Gale et al., 2007; Arthur et al., 2008; LaFollete and Schein, 2007; Lecompte et al., 2009). The assumption in the present work is that the hydraulic fracture has a penny-shape, a constant-height, or an ellipsoidal shape (Figures 3–6).

1.2 WORK SCOPE

The purpose of this work is to determine the extent of a potential damage zone in geologic formations above the pay zone during stimulation of gas shale reservoirs (Barnett shale, Marcellus shale, Fayetteville shale, and Haynesville shale). In this study, the fracture length, fracture height, and fracture width were determined for different volumes of fluid injection in different shale formations. The computations were based on three existing theories of fracture propagation, and the results from these models were compared to assess dependency of the predictions on the underlying theory. The study was based on the assumption that the hydraulic fracture has a penny-shape, a constant-height, or an ellipsoidal shape that is generated at the center of the shale layer during hydraulic fracturing and that the fracture lies along a single plane.
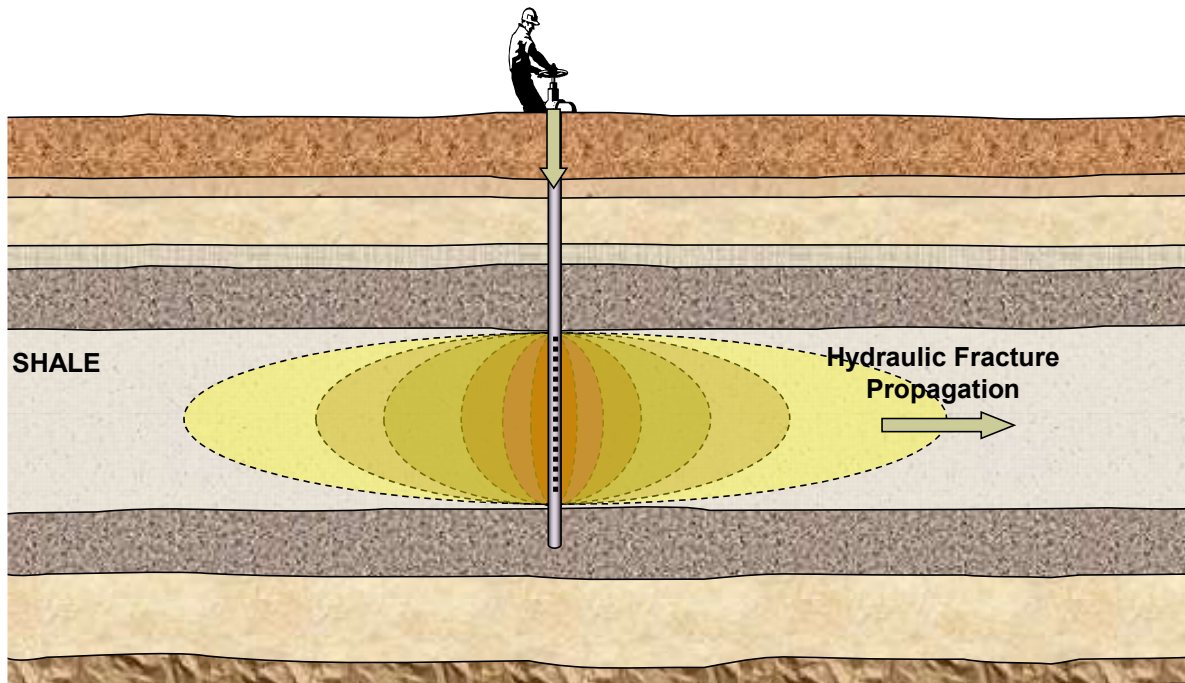
Figure 1: A schematic diagram of hydraulic fracture propagation.
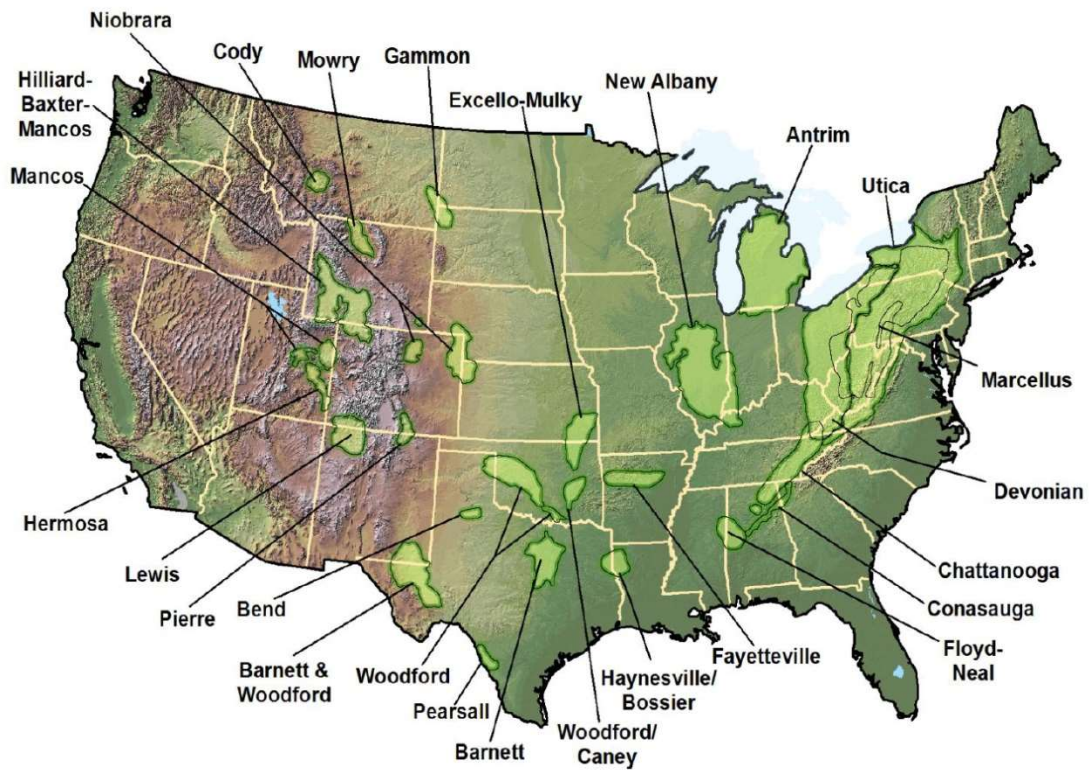
Figure 2: Location of major shale basins (DOE, 2009).

Table 1: Comparisons of four major gas shale basins (Gale et al., 2007; Arthur et al., 2008; LaFollete and Schein, 2007; Lecompte et al., 2009; DOE, 2010)

Gas Shale Basin	Barnett	Marcellus	Haynesville	Fayetteville
Estimated Basin Area (mi²)	5,000	95,000	9,000	9,000
Depth (ft)	6,500–8,500	4,000–8,500	10,500–13,500	1,000–7,000
Net Thickness (ft)	100–600	50–200	20–200	200
Depth to Base of Water (ft)	1,200	850	400	500
Organic Carbon (%)	5	3–12	2–4	4–10
Porosity (%)	4–5	8–10	6–10	2–8
Gas Content (SCF/ton)	300–350	60–120	100–330	60–220
Well Spacing (ac)	60–160	40–160	40–560	80–160
Gas In Place (TCF)	327	1,500	717	52
Reserves (TCF)	44	250–500	251	42
Estimates Gas Production (MCF/day/well)	338	3,100	625–1,800	530
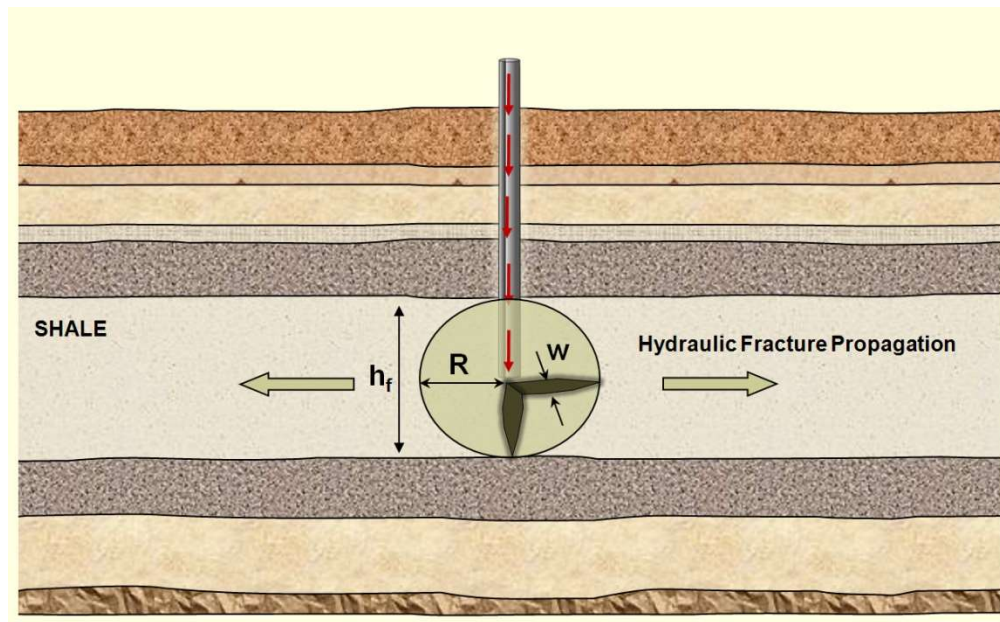
(a) Fracture limiting to the pay zone.
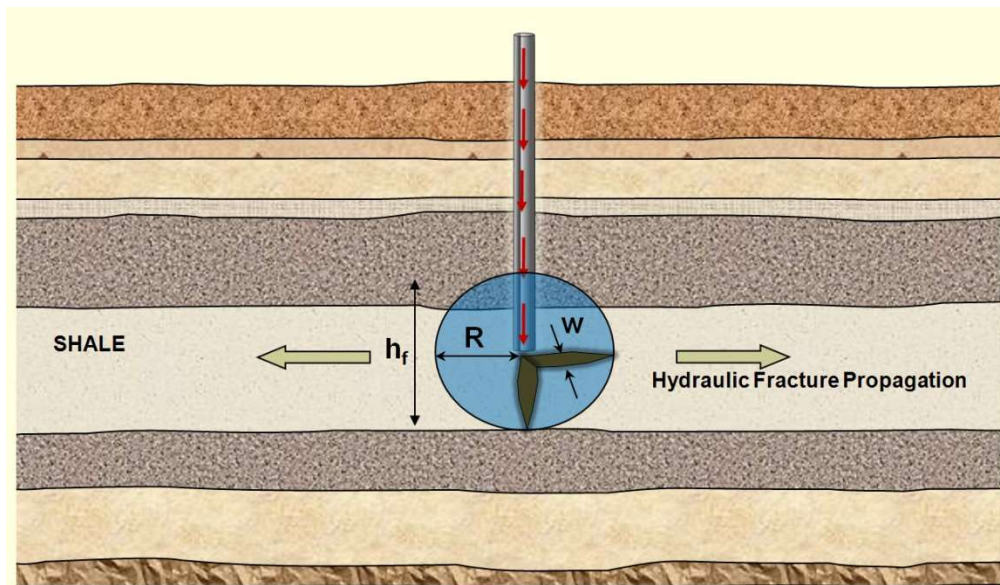
(b) Fracture beyond the pay zone.

Figure 3: Penny-shaped fracture.

2. **METHODOLOGY**

2.1 **FRACTURE MODELS**

The fracture models considered in this study, including their theoretical and geometric details, are described in Meyer (1989) and Meyer & Associates (2009). The computer code MFAST (Meyer & Associates, 2009) was used in this study. This computer code is capable of predicting how hydraulically induced fractures propagate in subsurface formations by using different fracture propagation theories. This code was used because of its capability to include simplified assumptions on fracture geometry. Two-dimensional (2-D) fractures based on the Perkins and Kern model (PKN) (Perkins and Kern, 1961; Nordgren, 1972), Geertsma-De-Klerk model (GDK) (Geertsma and De Klerk, 1969), and Ellipsoidal models were considered in this study. Figures 4, 5 and 6 illustrate the approximations of the PKN model, GDK model, and Ellipsoidal models. The differences between PKN, GDK and Ellipsoidal models are listed in Table 2. Ellipsoidal models exhibit some properties of the PKN and some properties of the GDK models, depending on the parameters used. In this study, the geometry of an ellipsoidal fracture was considered. When the aspect ratio is 1, the geometry of the ellipsoidal fracture reduces to radial solution (Figure 3). In the vertical Ellipsoidal model, the geometry of the vertical ellipsoidal fracture intersects the wellbore along the fracture height. More details on these models can be found elsewhere (Meyer & Associates, 2009).

Approximations of the PKN, GDK, and Ellipsoidal models were used in determining the extent of fractures (Meyer & Associates, 2009). The variables considered in the study are:

1. Fluid injection rate (q = 30 bpm and q = 120 bpm)

2. Injection volume (Q = 400,000 gal and Q = 1,000,000 gal)

3. Leakoff coefficient (C = 0.0015 ft/min$^{1/2}$)

4. Pay zone thickness (formation dependent)

In these simulations, the vertical extent of the fracture was not restricted to the reservoir thickness. Instead, the fractures were allowed to propagate in the vertical direction without any constraints. It was assumed that the vertical fracture propagation occurs towards the ground surface rather than propagating below the pay zone. This assumption will lead to a conservative estimate for the vertical propagation of hydraulic fractures toward the ground surface. The injection volumes assumed in this study are conservative estimates of typical fracturing operations involving multiple fractures stimulated using horizontal well configurations. In the case of Q = 1,000,000 gal, it is highly unlikely that one single fracture will propagate during such large-volume stimulations. Therefore, the assumed values of injection volumes are considered conservative estimates.
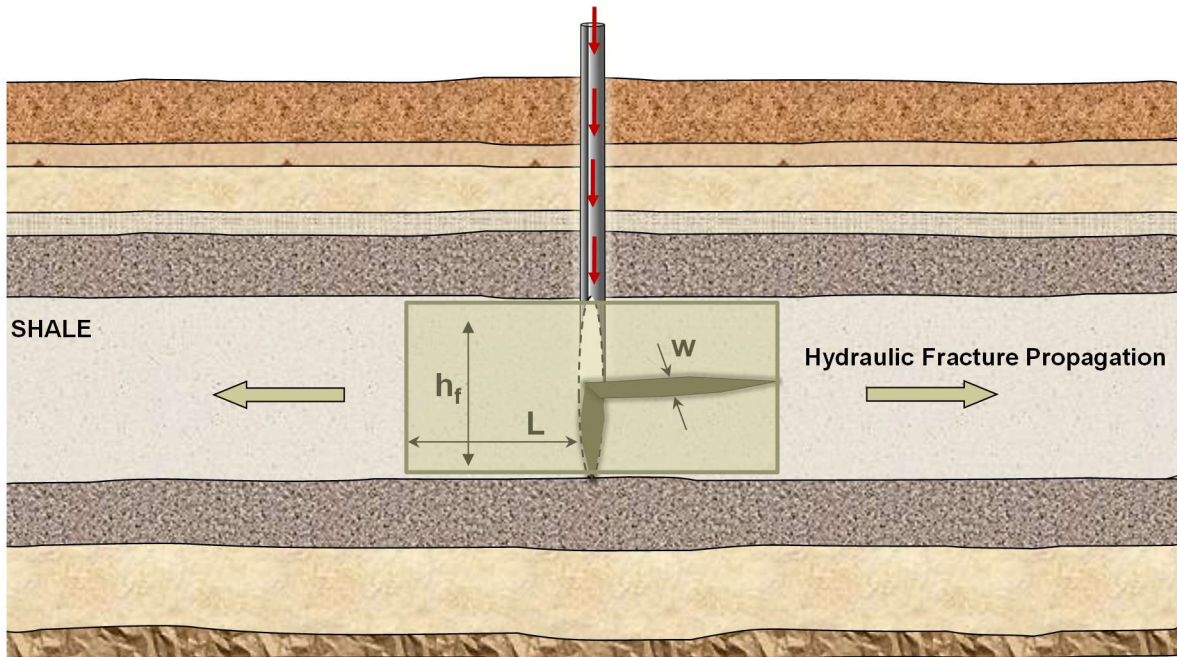
(a) Fracture limiting to the pay zone.
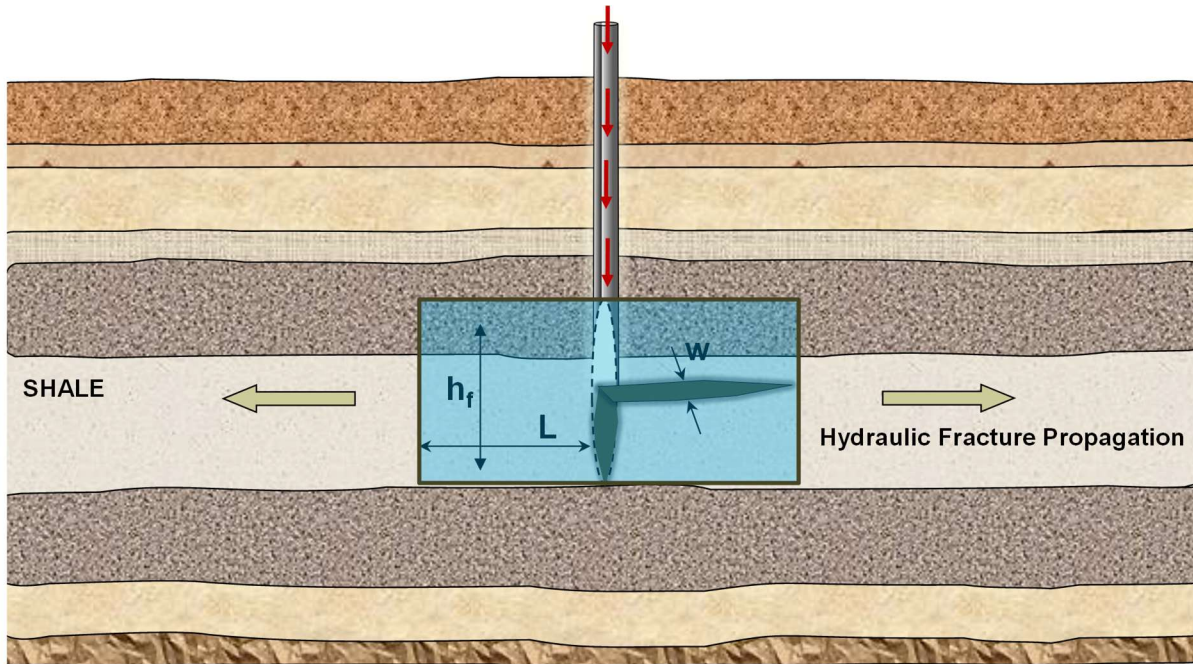
(b) Fracture beyond the pay zone.

Figure 4: PKN model.
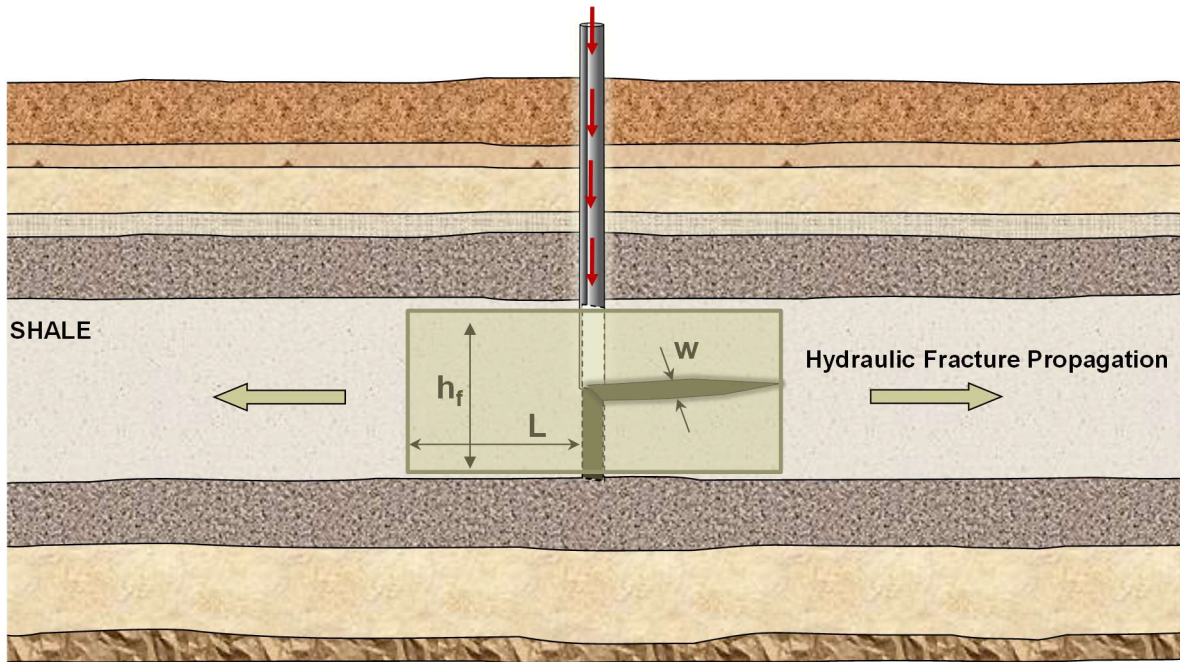
(a) Fracture limiting to the pay zone.
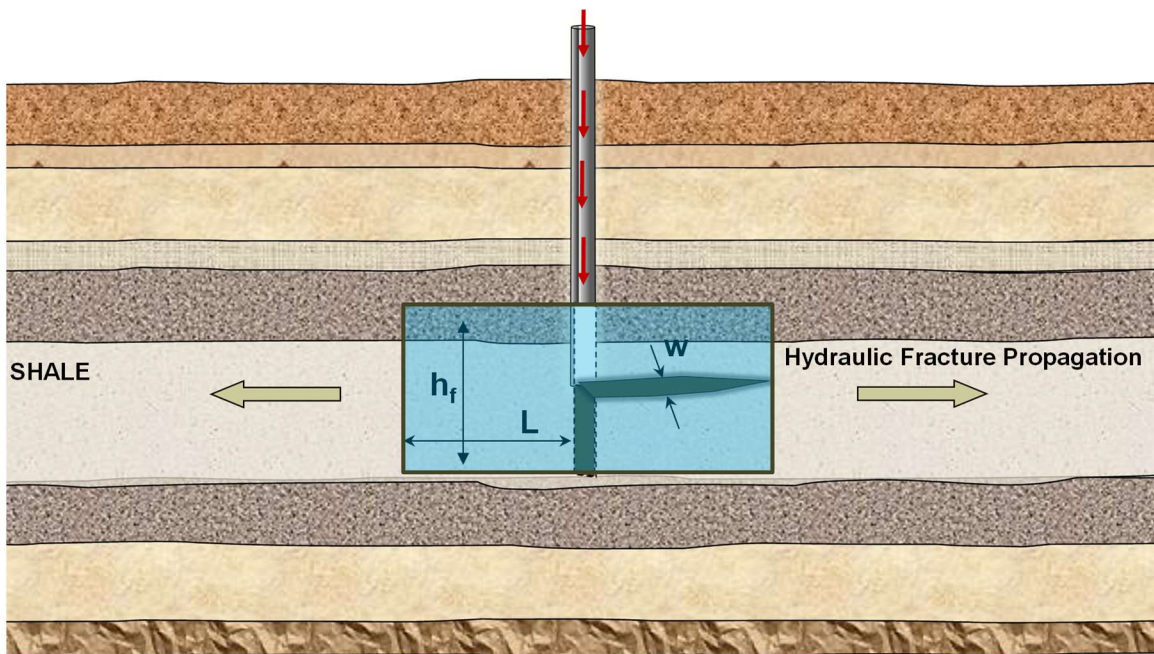
(b) Fracture beyond the pay zone.

Figure 5: GDK model.
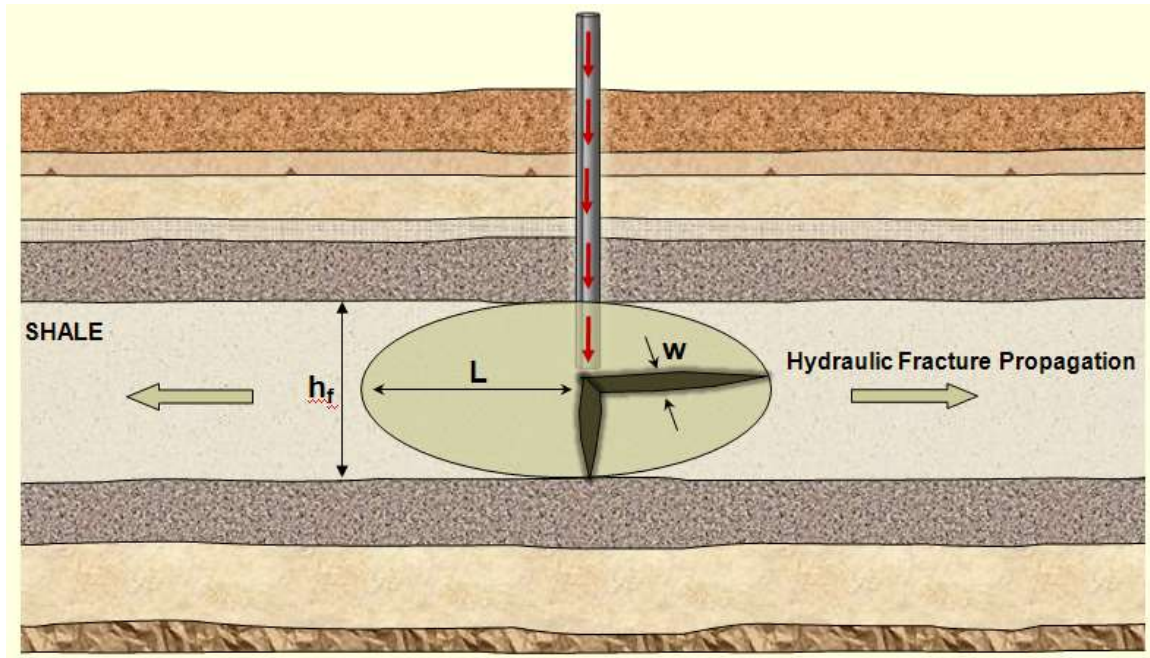
(a) Fracture limiting to the pay zone.
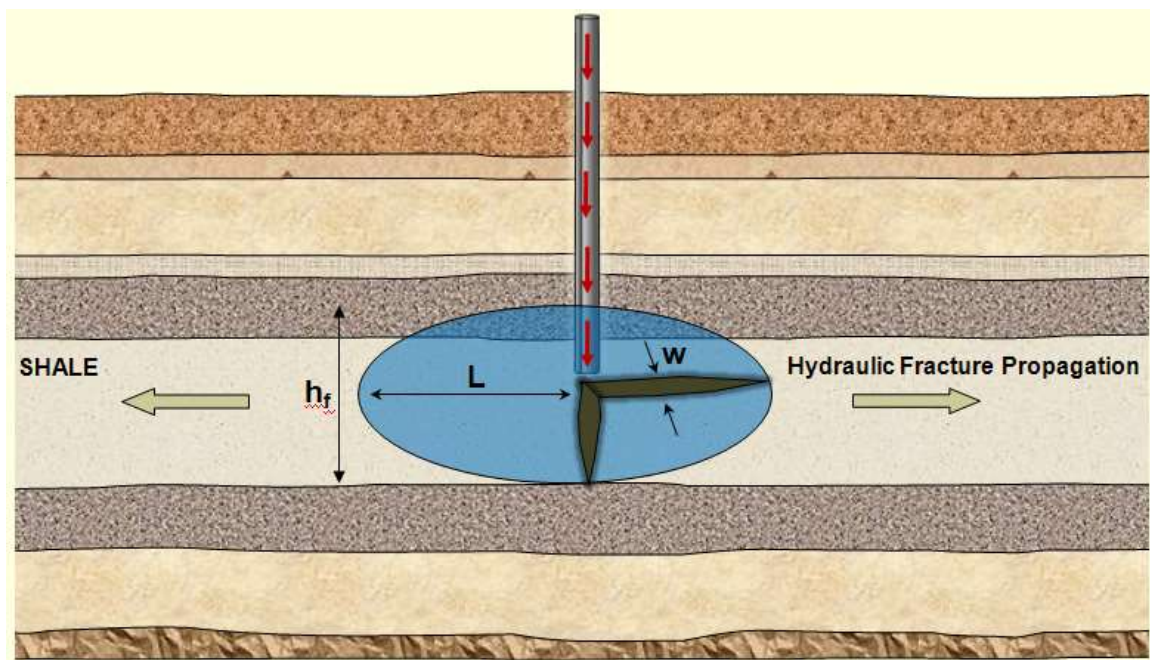
(b) Fracture beyond the pay zone.

Figure 6: Ellipsoidal model.

Model	PKN	GDK	Ellipsoidal
	Assumes vertical plane strain	Assumes horizontal plane strain	Horizontal or vertical ellipsoidal
Fracture	Constant fracture height geometric model, but differ by having an elliptically shaped width in the vertical plane	Constant fracture height geometric model with constant fracture width	Ellipsoidal width profile
Geometry	Vertically bounded geometry	Vertically unbounded geometry if fracture height is much greater than the fracture length or if slip occurs at the boundaries of pay zone i.e., at the lower and upper extremities	Ellipsoidal hydraulic fracture intersects wellbore
Applications	Mostly applicable when λ (aspect ratio) > 1	Mostly applicable when λ (aspect ratio) < 1	When λ (aspect ratio) = 1, fracture geometry leads to radial solution
Cross-section	Elliptical	Rectangular	Elliptical

2.2   MATHEMATICAL DETAILS OF FRACTURE PROPAGATION MODELS

This section presents constitutive equations for the fracture propagation models used (PKN, GDK and Ellipsoidal models) in the study. All models are based on the assumption of linear elastic, isotropic rocks. The width and length equations for these fracture propagation models with and without leak-off coefficients are presented in this section. The equations reported for one wing of the fracture is presented below (Meyer, 1986; Meyer and Hagel, 1989). Relationships between the fracture length (L) and the shear modulus (G) for these models can be found in the literature.

Perkins-Kern/Nordgren (PKN) model (Perkins and Kern, 1961; Nordgren, 1972)

As discussed in Table 2, the PKN model assumes a constant fracture height with vertical geometric width (Meyer, 1986) as shown in Figure 4(a). The fracture width is elliptical in the vertical plane and the model is mostly suitable for fractures with aspect ratio (λ = L/H) greater than 1 (Meyer, 1986). The width of the fracture at any position "s" in the PKN model is given as (Meyer, 1986):

$$W(x,s,t) = W_W(x,0,t)\left(1 - s^2\right)^{1/2}$$

(1)

where

$W(x, s, t)$ is the fracture width at any position $S\left(s = \dfrac{z}{H}\right)$

$W(x, 0, t)$ is the maximum fracture width at any position "x".

The width of the fracture in the PKN model is given as (Meyer, 1986):

$$W_W(x, 0, t) = \frac{\tau_{w0}(1 - v)}{G} H_w \Delta P(x, t) \tag{2}$$

The length and width for the fracture in the PKN model is shown below (Meyer, 1986):

$$L(t) = \frac{Q t^{1/2}}{2\pi C_{leak} H_p} \tag{3}$$

$$W_w(t) = a\left[\frac{1 - v}{G} K_a (Q/H_w)^{n'} (QH_w/C_{leak} H_p)\right]^{\frac{1}{2n'+2}\frac{1}{t^{3n'+4}}} \tag{4}$$

where

$a = \left[3^{n'} \Gamma_{w0} / (\Gamma_p \Gamma_f \pi)\right]^{1/(2n'+2)}$

$\Gamma_{w0} = 1.0$

$\Gamma_p \cong 1/(2n'+2)$

$\Gamma_f \cong 3\pi/16$

C_{leak} = Total leak-off coefficient

G = Shear Modulus, $G = \dfrac{E}{2(1 - v)}$

E = Elastic modulus

Hp = Pay zone height

Hw = Total fracture height at the wellbore

Ka = Apparent consistency index

n' = Slurry flow behavior index

Q = Total flow rate

ι = Poisson's ratio

Geertsma-Deklerk (GDK) model (Geertsma and De Klerk, 1969)

The GDK model assumes a constant fracture height in a horizontal plane (Meyer, 1986) as shown in Figure 5. The fracture shape is rectangular with constant width. This model is mostly suitable for fractures with aspect ratio ($\lambda = L/H$) less than 1. Table 2 presents the differences between the PKN, GDK, and Ellipsoidal models. For the GDK model, the width of the fracture at any position (s') is given as (Meyer, 1986):

$$W(s',t) = W_w(t)\left(1 - s'^2\right)^{1/2}$$ (5)

where

$W(s',t)$ is the width at any position, s' $\left(s' = \dfrac{x}{L(t)}\right)$

$W_w(t)$ is the maximum fracture width at the wellbore $\left(W_w(t) = W(0,t)\right)$

The width-opening pressure relationship is the major difference in PKN and GDK (Meyer, 1986) models. More details can be found elsewhere (Meyer, 1986; Meyer and Hagel, 1989). The width-opening pressure relationship for the GDK model is given by (Meyer, 1986):

$$W_w(t) = \frac{2\tau_{w0}(1-v)}{G}L(t)\Delta P(0,t)$$ (6)

The length and width for the GDK model is presented below (Meyer, 1986):

$$L(t) = \frac{Qt^{1/2}}{2\pi\, C_{leak}\, H_p}$$ (7)

$$W_w(t) = a\left[\frac{1-v}{G}K_a\left(\frac{Q}{H_w}\right)^{n'+2}\left(\frac{Q}{C_{leak}H_p}\right)^2\right]^{\frac{1}{2(n'+2)}}t^{\frac{1}{2n'+2}}$$ (8)

where

$$a = \left[\frac{3^{n'}\tau_{w0}}{\left(\tau_p\tau_f\pi^2\right)}\right]^{\frac{1}{(2n'+2)}}$$

Ellipsoidal Fracture Model

The Ellipsoidal fracture model considers a variable fracture height with characteristics of both, the PKN and the GDK models as shown in Figure 6. It considers fracture propagation in both, horizontal and vertical directions. If the aspect ratio is greater than 1, the model solution approaches the PKN model. Otherwise, it approaches the GDK model. More details can be found elsewhere (Meyer, 1986; Meyer, 1989; Meyer and Hagel, 1989). Equation 9 provides the fracture width at any position, *r* (Meyer, 1986):

$$W(r,t) = W(0,t)\left[1 - (r/R)^2\right]^{1/2} \tag{9}$$

where:

$W(r,t)$ is the width at any position, r

$W(0,t)$ is the maximum wellbore width

R is the facture radius at any time, t

The width and radius for the Elliptical model is shown below (Meyer, 1986):

$$W_w(t) = \left[a\frac{1-v}{G}K_a Q^{\frac{n'+2}{2}} C_{leak}^{\frac{n'-2}{2}} \right]^{\frac{1}{2n'+2}} t^{\frac{2-n'}{8n'+8}} \tag{10}$$

$$R(t) = \left[\frac{Qt^{1/2}}{\pi^2 C_{leak}} \right]^{1/2} \tag{11}$$

where

$$a = \left[\frac{4(3/2)^{n'} \Gamma_{w0}}{\Gamma_f \Gamma_p \pi^{2-n'}} \right]^{\frac{1}{2n'+2}}$$

3. EVALUATION OF INDIVIDUAL SHALE BASINS

3.1 BARNETT SHALE

The Barnett shale is one of the thickest shale basins in the United States. In this study, the Barnett shale basin was selected to study the fracture length, fracture height, and fracture width for different pay zone thicknesses and injection volumes. Properties such as gas content, gas-in-place, formation depth, and depths to the groundwater table were evaluated based on published information (Gale et al., 2007; DOE, 2009). Table 3 shows the properties of the Barnett shale used in the study. In order to investigate the influence of properties of the Barnett shale basin on the extent of the potential damage zone, approximations of the PKN, GDK, and Ellipsoidal (Aspect Ratio = 1) models were considered. Two-dimensional models were used to simulate hydraulic fracturing as shown in Figure 3. Computations were performed using MFAST (Meyer & Associates, 2009). In these simulations, the vertical extent of the fracture was not restricted to the reservoir thickness. Instead, the fractures were allowed to propagate in the vertical direction without any constraints.

Figure 7 and Figure 8 show variations of fracture length and fracture width, depending on the amount of injected fluid (for q = 30 bpm), respectively. Figure 9 and Figure 10 show the variations of fracture length and fracture width with the injection period (injection time). Table 4 compares fracture parameters from the three fracture propagation models (PKN, GDK and Ellipsoidal models) for different fluid injection rates and fluid injection volumes in the Barnett shale formation. In these simulations, the vertical extent of the fracture was not restricted to the reservoir thickness. Instead, the fractures were allowed to propagate in the vertical direction without any constraints. Results show that both fracture length and fracture height increase with the fluid injection volume. Also, an increase in the fracture length and fracture height was observed with an increase in the fluid injection rate.

Table 3: Properties of Barnett shale used in the modeling study

Property	Unit of Measure	Barnett
Young's Modulus, E	(psi)	4.80E+06
Fracture Toughness	(psi-in$^{1/2}$)	850
Poisson's Ratio	--	0.25
Payzone Height	(ft)	300–500
Ellipsoidal Aspect Ratio	--	1
Injection Rate (2-wings)	(bpm)	30 and 120
Flow Behavior Index - n'	--	0.6
Consistency Index - K'	(lbf-s$^{n'/ft2}$)	0.02
Leakoff Coefficient	(ft/min$^{0.5}$)	0.0015
Spurt Loss Coefficient	(gal/ft^2)	0
Total Volume Injected	(gal)	1,000,000 and 400,000
Max Proppant Concentration	(lbm/gal)	3

Figure 7: Variation of fracture length with the amount of fluid injection in the Barnett shale for q = 30 bpm. This figure was generated by MFAST (Meyer & Associates, 2009).
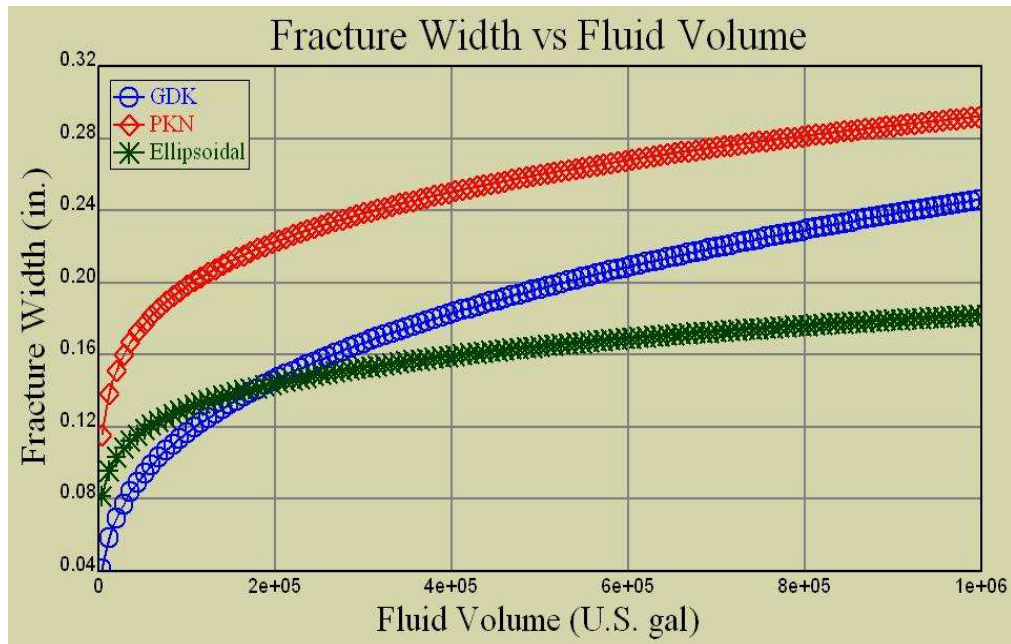
Figure 8: Variation of fracture width with the amount of fluid injection in the Barnett shale for q = 30 bpm. This figure was generated by MFAST (Meyer & Associates, 2009).
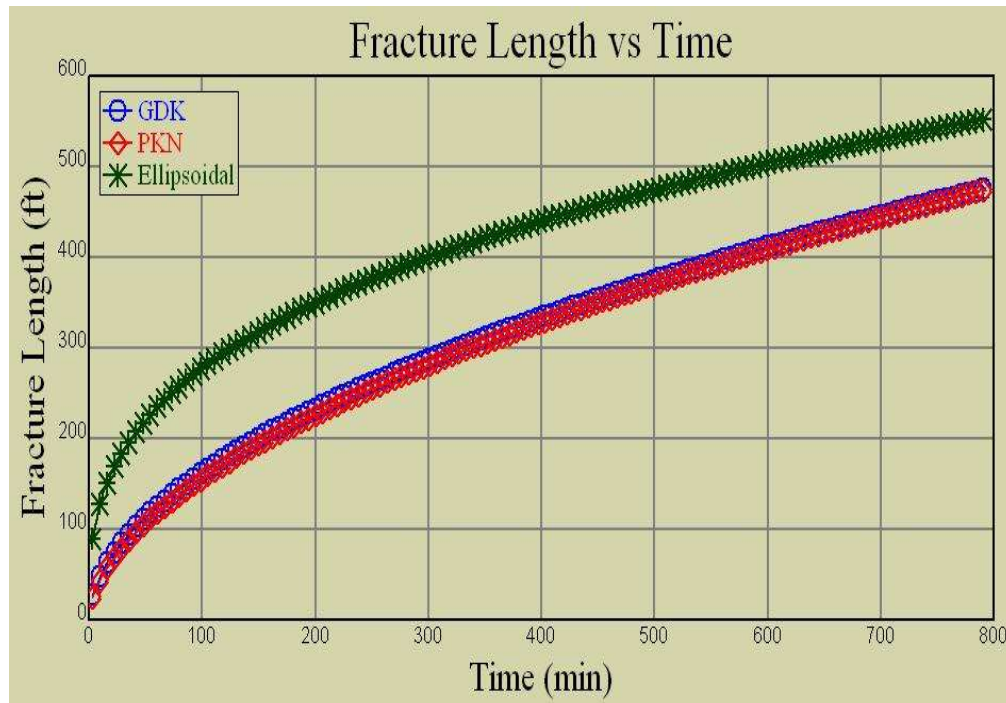
Figure 9: Variation of fracture length with fluid injection time in the Barnett shale for q = 30 bpm. This figure was generated by MFAST (Meyer & Associates, 2009).
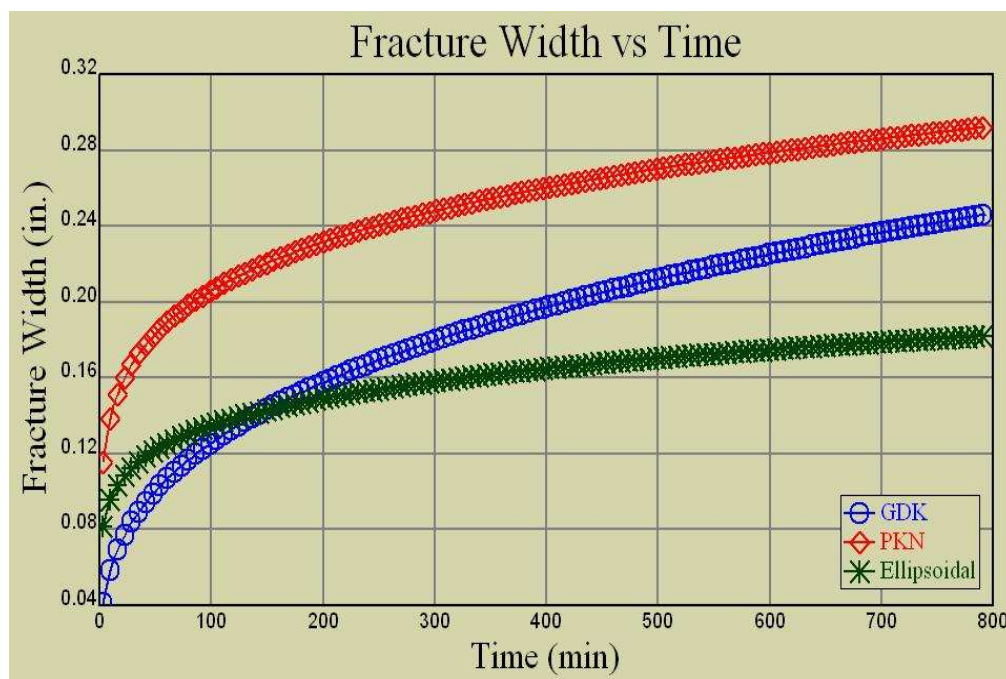
Figure 10: Variation of fracture width with fluid injection time in the Barnett shale for q = 30 bpm. This figure was generated by MFAST (Meyer & Associates, 2009).

Table 4: Influence of fluid injection rates and injection volumes on computed fracture geometry in the Barnett shale

BARNETT SHALE						
	Q = 1 M gal, q = 30 bpm, Leakoff = 0.0015 ft/min$^{0.5}$			Q = 400,000 gal, q = 30 bpm, Leakoff = 0.0015 ft/min$^{0.5}$		
Parameters	GDK	PKN	Ellipsoidal	GDK	PKN	Ellipsoidal
Length (ft) - 2L	950.80	950.43	1105.73	740.41	739.39	864.59
Height (ft)	951.00	950.00	1105.73	740.40	739.40	864.59
Max. Well Width (in.)	0.25	0.37	0.23	0.22	0.33	0.21
Ave. Well Width (in.)	0.25	0.29	0.18	0.22	0.26	0.16
Ave. Frac. Width (in.)	0.19	0.21	0.15	0.17	0.19	0.14
Net Pressure (psi)	70.39	83.54	95.68	80.99	96.23	109.93
Pumping Time (min)	793.65	793.65	793.65	317.46	317.46	317.46
	Q = 1 M gal, q = 120 bpm, Leakoff = 0.0015 ft/min$^{0.5}$			Q = 400,000 gal, q = 120 bpm, Leakoff = 0.0015 ft/min$^{0.5}$		
Parameters	GDK	PKN	Ellipsoidal	GDK	PKN	Ellipsoidal
Length (ft) - 2L	1229.05	1224.21	1452.50	931.03	924.99	1107.58
Height (ft)	1229.10	1224.30	1452.50	931.00	925.00	1107.58
Max. Well Width (in.)	0.36	0.54	0.34	0.31	0.48	0.30
Ave. Well Width (in.)	0.36	0.42	0.26	0.31	0.37	0.24
Ave. Frac. Width (in.)	0.28	0.30	0.22	0.25	0.27	0.20
Net Pressure (psi)	78.51	93.55	106.59	91.75	109.73	124.25
Pumping Time (min)	198.41	198.41	198.41	79.37	79.37	79.37

3.2   MARCELLUS SHALE

Marcellus shale is widely found in the United States in West Virginia, Ohio, Maryland, New York, Pennsylvania, and Kentucky (DOE, 2009). In this study, Marcellus shale was selected to evaluate the fracture length, fracture height, and fracture width for different pay zone thicknesses and fluid injection volumes. Gas content, gas-in-place, formation depth, and depth to groundwater table were estimated based on literature (Arthur et al., 2008; DOE, 2009). Table 5 shows the list of shale properties used in the modeling study to evaluate fracture geometry in Marcellus shale. Similar to Barnett shale, 2-D models—PKN, GDK, and Ellipsoidal (Aspect Ratio = 1) models—were considered. Computations were performed using MFAST (Meyer & Associates, 2009). In these simulations, the vertical extent of the fracture was not restricted to the reservoir thickness. Instead, the fractures were allowed to propagate in the vertical direction without any constraints.

Figure 11 and Figure 12 show changes in fracture length and fracture width with the amount of injected fluid (for q = 30 bpm) in the Marcellus Shale by using fracture propagation models of PKN, GDK and Ellipsoidal (Aspect Ratio = 1). Figure 13 and Figure 14 show variations of fracture length and fracture width as a function of injection time. Table 6 compares fracture parameters from the three fracture propagation models (PKN, GDK and Ellipsoidal) for different fluid injection rates and fluid injection volumes in the Marcellus shale formation. Results show an increase in the fracture length and fracture height with an increase in the injection volume and injection rate.

Table 5: Properties of Marcellus shale used in the modeling study

Property	Unit of Measure	Marcellus
Young's Modulus, E	(psi)	1.05E+06
Fracture Toughness	$(\text{psi-in}^{1/2})$	850
Poisson's Ratio	--	0.25
Payzone Height	(ft)	50–300
Ellipsoidal Aspect Ratio	--	1
Injection Rate (2-wings)	(bpm)	30 and 120
Flow Behavior Index - n'	--	0.6
Consistency Index - K'	$(\text{lbf-s}^{n'/\text{ft2}})$	0.02
Leakoff Coefficient	$(\text{ft/min}^{0.5})$	0.0015
Spurt Loss Coefficient	(gal/ft^2)	0
Total Volume Injected	(gal)	1,000,000 and 400,000
Max Proppant Concentration	(lbm/gal)	3

Figure 11: Variation of fracture length with the amount of fluid injection in Marcellus shale for q = 30 bpm. This figure was generated by MFAST (Meyer & Associates, 2009).
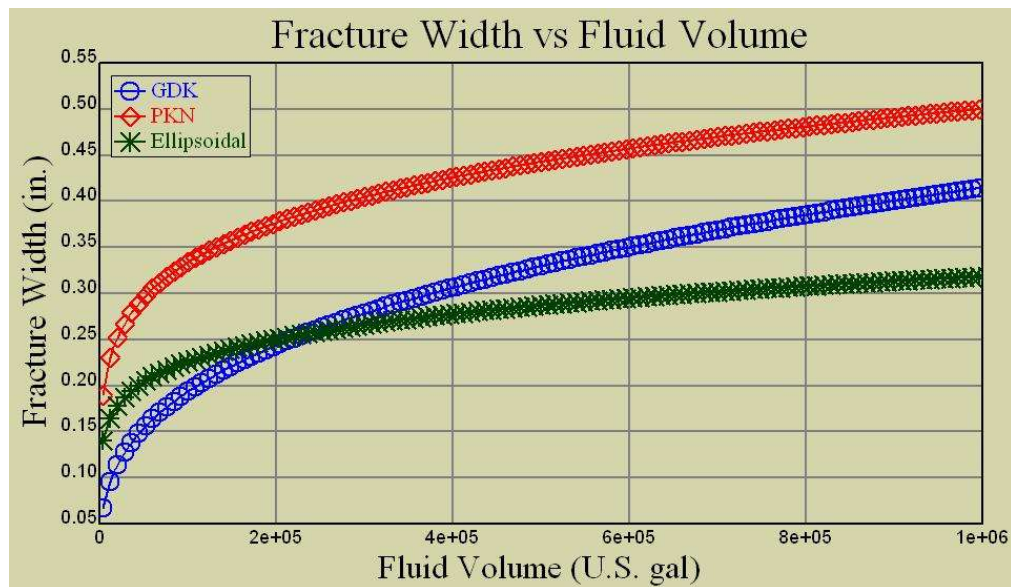
Figure 12: Variation of fracture width with the amount of fluid injection in Marcellus shale for q = 30 bpm. This figure was generated by MFAST (Meyer & Associates, 2009).
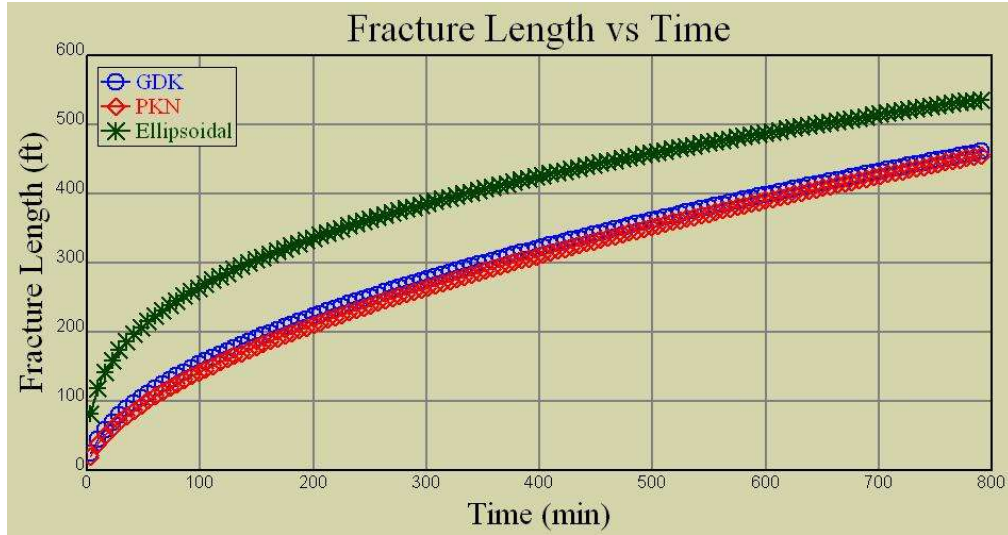
Figure 13: Variation of fracture length over injection time in the Marcellus formation for q = 30 bpm. This figure was generated by MFAST (Meyer & Associates, 2009).
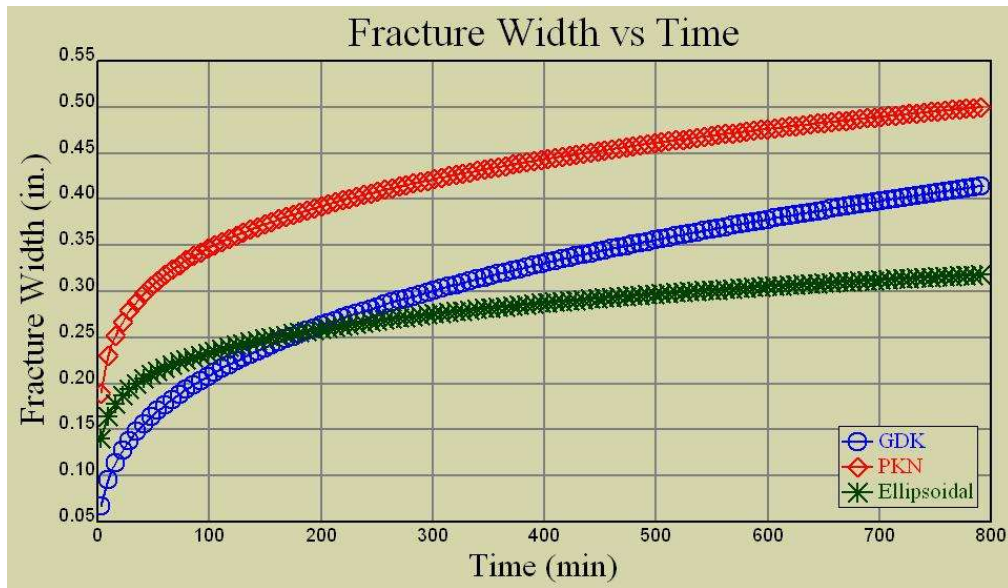
Figure 14: Variation of fracture width over injection time in the Marcellus formation for q = 30 bpm. This figure was generated by MFAST (Meyer & Associates, 2009).

Table 6: Influence of fluid injection rates and injection volumes on computed fracture geometry in the Marcellus shale

	Marcellus Shale					
	Q = 1 M gal, q = 30 bpm, Leakoff = 0.0015 ft/min$^{0.5}$			Q = 400,000 gal, q = 30 bpm, Leakoff = 0.0015 ft/min$^{0.5}$		
Parameters	GDK	PKN	Ellipsoidal	GDK	PKN	Ellipsoidal
Length (ft) - 2L	919.24	913.82	1073.51	707.63	701.77	830.54
Height (ft)	919.00	913.80	1073.51	707.60	701.70	830.54
Max. Well Width (in.)	0.41	0.64	0.41	0.37	0.57	0.36
Ave. Well Width (in.)	0.41	0.50	0.32	0.37	0.45	0.28
Ave. Frac. Width (in.)	0.32	0.37	0.27	0.29	0.33	0.24
Net Pressure (psi)	26.71	32.52	34.55	30.90	37.72	39.94
Pumping Time (min)	793.65	793.65	793.65	317.46	317.46	317.46
	Q = 1 M gal, q = 120 bpm, Leakoff = 0.0015 ft/min$^{0.5}$			Q = 400,000 gal, q = 120 bpm, Leakoff = 0.0015 ft/min$^{0.5}$		
Parameters	GDK	PKN	Ellipsoidal	GDK	PKN	Ellipsoidal
Length (ft) - 2L	1140.97	1124.91	1356.29	849.67	833.76	1015.64
Height (ft)	1140.90	1124.90	1356.29	849.60	833.70	1015.64
Max. Well Width (in.)	0.58	0.89	0.57	0.51	0.78	0.50
Ave. Well Width (in.)	0.58	0.70	0.45	0.51	0.61	0.39
Ave. Frac. Width (in.)	0.45	0.51	0.38	0.40	0.45	0.33
Net Pressure (psi)	30.08	36.74	39.24	35.46	43.52	46.23
Pumping Time (min)	198.41	198.41	198.41	79.37	79.37	0.42

3.3   FAYETTEVILLE SHALE

Fayetteville shale is found in the United States in the state of Arkansas (DOE, 2009). In this study, Fayetteville shale was selected to evaluate the fracture length, fracture height, and fracture width for different pay zone thicknesses and fluid injection volumes. Table 7 shows the properties of shale used in the evaluation of the Fayetteville shale. These properties were estimated on the basis of available literature on Fayetteville shale (DOE, 2009; Arthur et al., 2008; Gale et al., 2007). As in the previous cases, PKN, GDK, and Ellipsoidal (Aspect Ratio = 1) models were considered. Computations were performed using MFAST (Meyer & Associates, 2009). In these simulations, the vertical extent of the fracture was not restricted to the reservoir thickness. Instead, the fractures were allowed to propagate in the vertical direction without any constraints.

Figure 15 and Figure 16 show the influence of fluid injection volume (for q = 30 bpm) on fracture length and fracture width. Results show an increase in fracture length and fracture width with an increase in the fluid injection volume. Figure 17 and Figure 18 show the influence of fluid injection rates on the fracture length and fracture width, respectively. Results show an increase in fracture length and fracture width with an increase in the fluid injection rates. Table 8 shows computed values of fracture parameters for the fracture propagation models (PKN, GDK, and Ellipsoidal) considered in this study.

Table 7: Properties of Fayetteville shale used in the modeling study

Property	Unit of Measure	Fayetteville
Fracture Toughness	(psi-in$^{1/2}$)	850
Poisson's Ratio	--	0.25
Payzone Height	(ft)	20–200
Ellipsoidal Aspect Ratio	--	1
Injection Rate (2-wings)	(bpm)	30 and 120
Flow Behavior Index - n'	--	0.6
Consistency Index - K'	(lbf-s$^{n'/ft2}$)	0.02
Leakoff Coefficient	(ft/min$^{0.5}$)	0.0015
Spurt Loss Coefficient	(gal/ft^2)	0
Total Volume Injected	(gal)	1,000,000 and 400,000
Max Proppant Concentration	(lbm/gal)	3

Figure 15: Variation of fracture length with fluid volume in the Fayetteville shale for q = 30 bpm. This figure was generated by MFAST (Meyer & Associates, 2009).

Figure 16: Variation of fracture width with fluid volume in the Fayetteville shale for q = 30 bpm. This figure was generated by MFAST (Meyer & Associates, 2009).
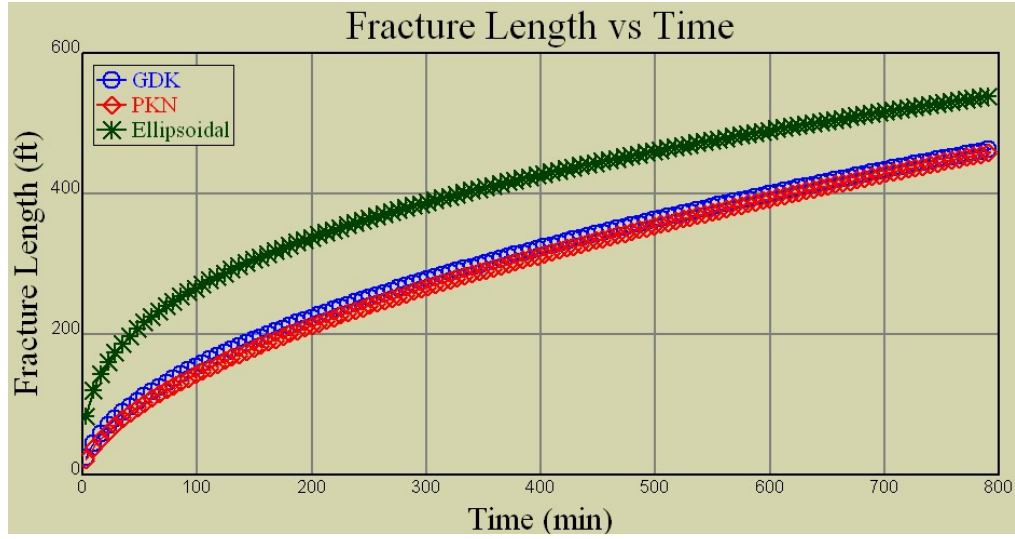
Figure 17: Variation of fracture length with fluid injection time in the Fayetteville shale for q = 30 bpm. This figure was generated by MFAST (Meyer & Associates, 2009).
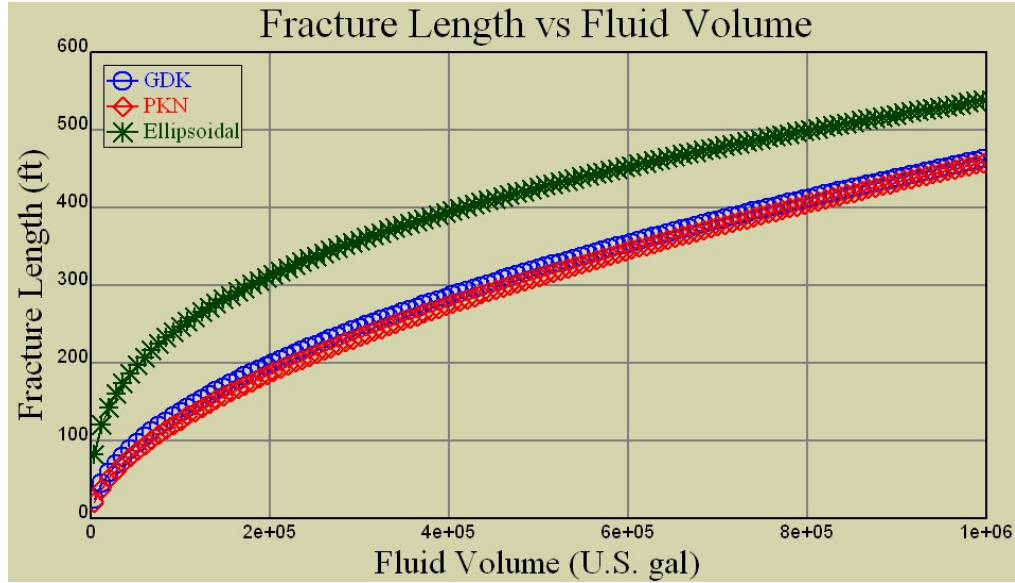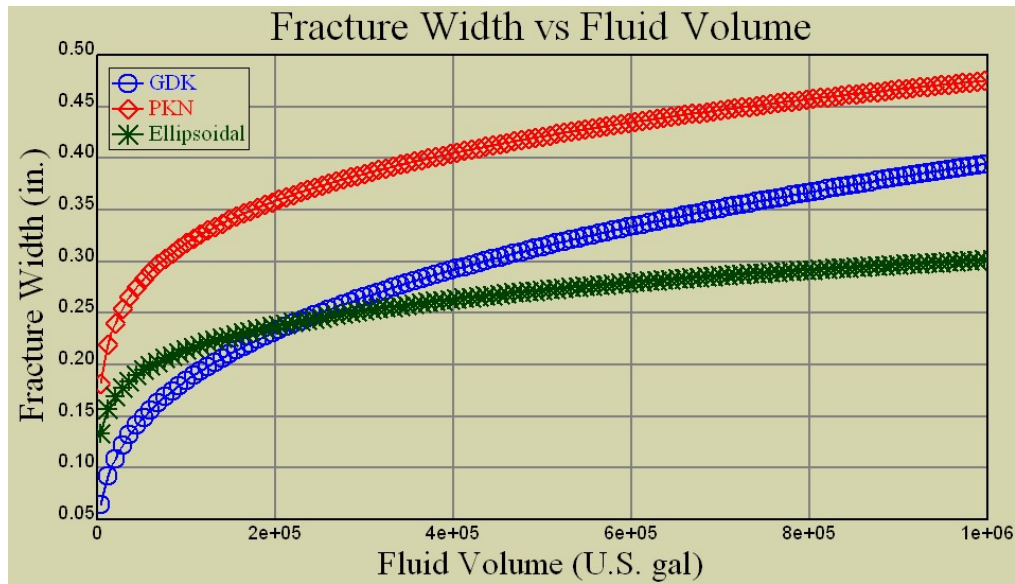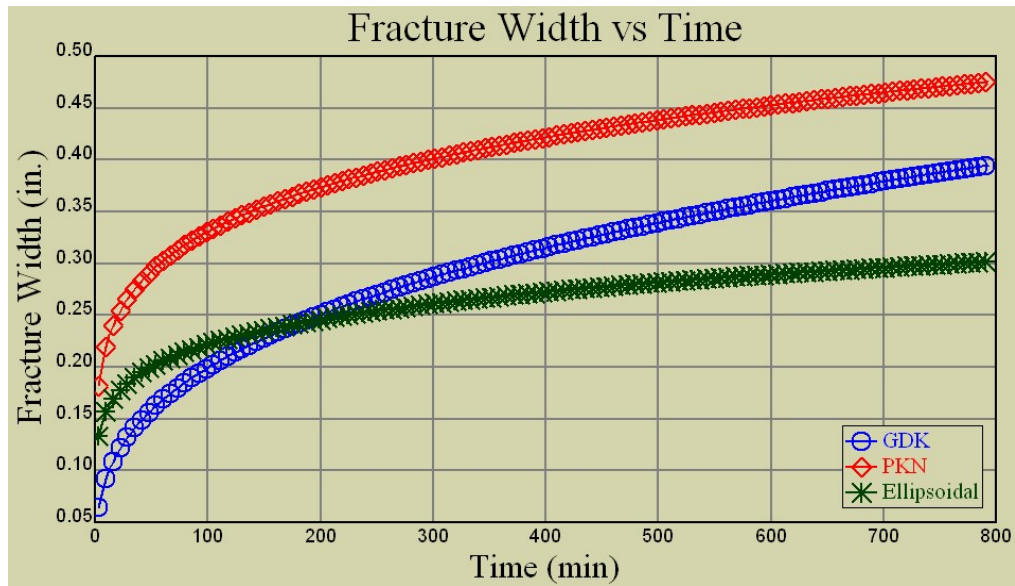

Figure 18: Variation of fracture width with fluid injection time in the Fayetteville shale for q = 30 bpm. This figure was generated by MFAST (Meyer & Associates, 2009).

Table 8: Influence of fluid injection rates and injection volumes on computed fracture geometry in the Fayetteville shale

FAYETTEVILLE SHALE						
	Q = 1 M gal, q = 30 bpm, Leakoff = 0.0015 ft/min$^{0.5}$			Q = 400,000 gal, q = 30 bpm, Leakoff = 0.0015 ft/min$^{0.5}$		
Parameters	**GDK**	**PKN**	**Ellipsoidal**	**GDK**	**PKN**	**Ellipsoidal**
Length (ft) - 2L	922.64	918.07	1077.32	711.20	706.11	834.52
Height (ft)	922.70	918.10	1077.32	711.20	706.00	834.52
Max. Well Width (in.)	0.39	0.61	0.38	0.35	0.54	0.34
Ave. Well Width (in.)	0.39	0.48	0.30	0.35	0.42	0.27
Ave. Frac. Width (in.)	0.31	0.35	0.26	0.28	0.31	0.23
Net Pressure (psi)	28.99	35.16	37.72	33.52	40.75	43.57
Pumping Time (min)	793.65	793.65	793.65	317.46	317.46	317.46
	Q = 1 M gal, q = 120 bpm, Leakoff = 0.0015 ft/min$^{0.5}$			Q = 400,000 gal, q = 120 bpm, Leakoff = 0.0015 ft/min$^{0.5}$		
Parameters	**GDK**	**PKN**	**Ellipsoidal**	**GDK**	**PKN**	**Ellipsoidal**
Length (ft) - 2L	1752.29	1649.77	2131.50	857.70	843.05	1025.28
Height (ft)	1752.20	1649.80	2131.51	857.80	843.10	1025.28
Max. Well Width (in.)	0.67	1.02	0.67	0.49	0.74	0.48
Ave. Well Width (in.)	0.67	0.80	0.53	0.49	0.58	0.37
Ave. Frac. Width (in.)	0.52	0.59	0.45	0.38	0.43	0.32
Net Pressure (psi)	25.79	32.86	33.73	38.44	47.01	50.34
Pumping Time (min)	198.41	198.41	198.41	79.37	79.37	79.37

3.4   HAYNESVILLE SHALE

Haynesville shale is found in the United States in Texas and Louisiana (DOE, 2009). In this study, Haynesville shale was selected to evaluate the fracture length, fracture height, and fracture width for different pay zone thicknesses and fluid injection volumes. Table 9 shows the properties of Haynesville shale basin in comparison to other shale formations. Basin characteristics include general information such as areal extent, depth, thickness, gas content, gas reserves, gas-in-place, depth to groundwater table, and porosity. The properties such as pay zone thickness, elastic modulus, fracture toughness, injection volume, and injection rate used in the study are presented in Table 9 (Lecompte et al., 2009; DOE, 2009). Computations were performed using MFAST (Meyer & Associates, 2009). In these simulations, the vertical extent of the fracture was not restricted to the reservoir thickness. Instead, the fractures were allowed to propagate in the vertical direction without any constraints.

Figure 19 and Figure 20 show the variation of fracture length and fracture width with the amount of injected fluid (for q = 30 bpm) in the Haynesville shale. Figure 21 and Figure 22 show variations in fracture length and fracture width over time in Haynesville for fracture propagation models—PKN, GDK, and Ellipsoidal (Aspect Ratio = 1)— considered in this study. Table 10 presents the numerical values of fracture characteristics obtained using these fracture propagation models. Results from Table 10 and Figures 20 through 22 show an increase in the fracture length and fracture width with an increase in fluid injection volume and fluid injection rate.

Table 9: Properties of Haynesville shale used in the modeling study

Property	Unit of Measure	Haynesville
Young's Modulus, E	(psi)	2.00E+06
Fracture Toughness	(psi-in$^{1/2}$)	850
Poisson's Ratio	--	0.25
Payzone Height	(ft)	50–100
Ellipsoidal Aspect Ratio	--	1
Injection Rate (2-wings)	(bpm)	30 and 120
Flow Behavior Index - n'	--	0.6
Consistency Index - K'	(lbf-s$^{n'/ft2}$)	0.02
Leakoff Coefficient	(ft/min$^{0.5}$)	0.0015
Spurt Loss Coefficient	(gal/ft^2)	0
Total Volume Injected	(gal)	1,000,000 and 400,000
Max Proppant Concentration	(lbm/gal)	3

Figure 19: Variation of fracture length with fluid volume in the Haynesville shale for q = 30 bpm. This figure was generated by MFAST (Meyer & Associates, 2009).

Figure 20: Variation of fracture width with fluid volume in the Haynesville shale for q = 30 bpm. This figure was generated by MFAST (Meyer & Associates, 2009).

Figure 21: Variation of fracture length with fluid injection time in the Haynesville shale for q = 30 bpm. This figure was generated by MFAST (Meyer & Associates, 2009).
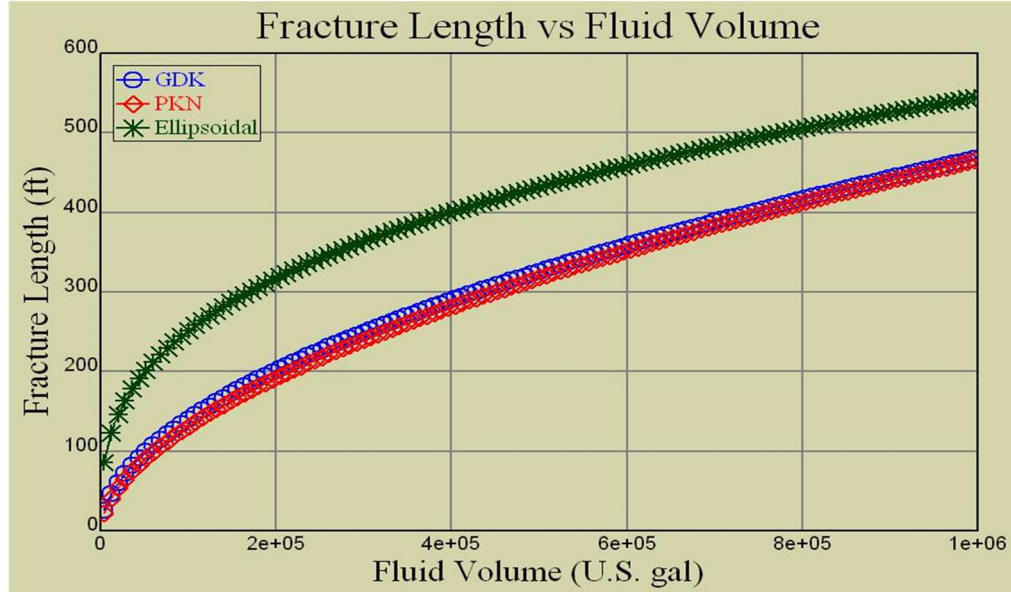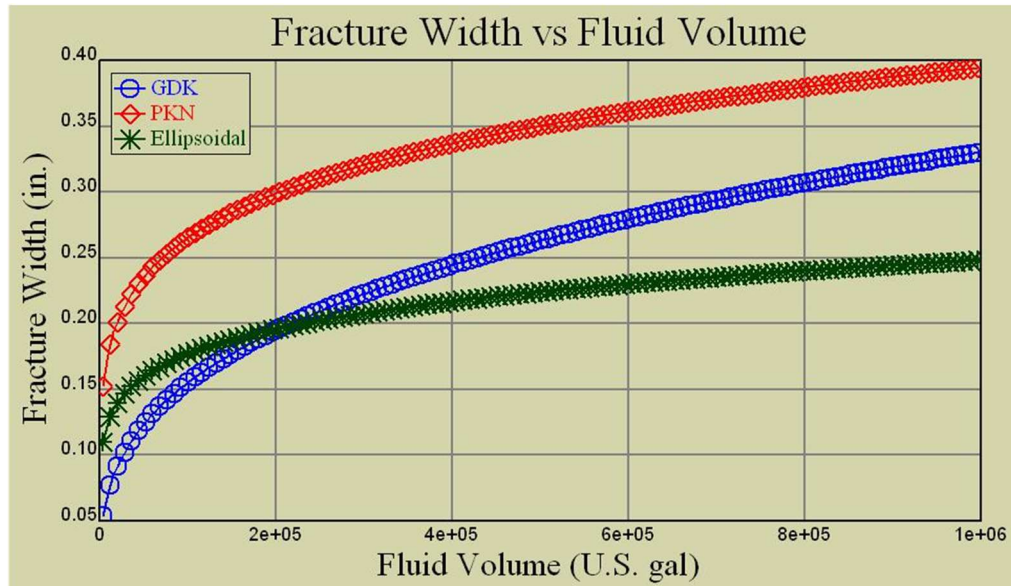

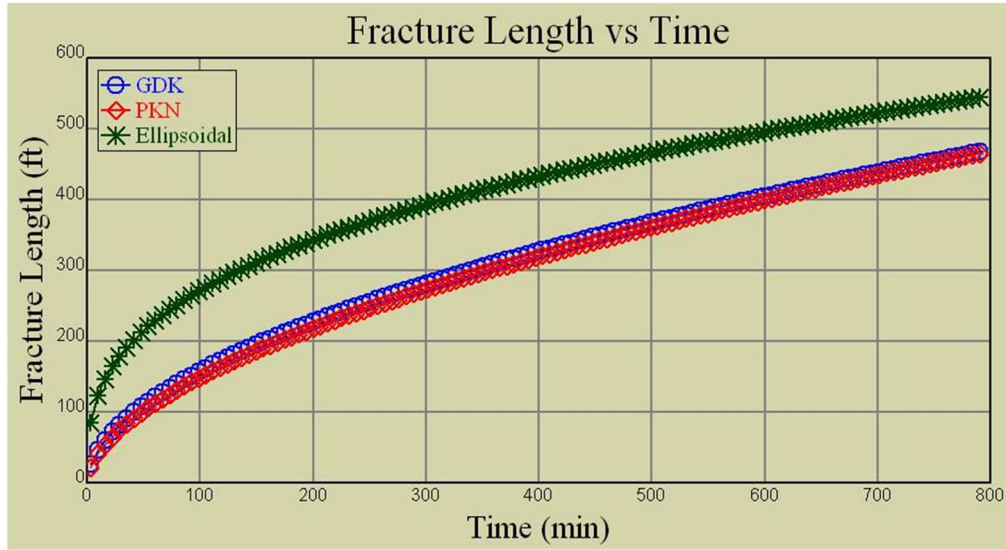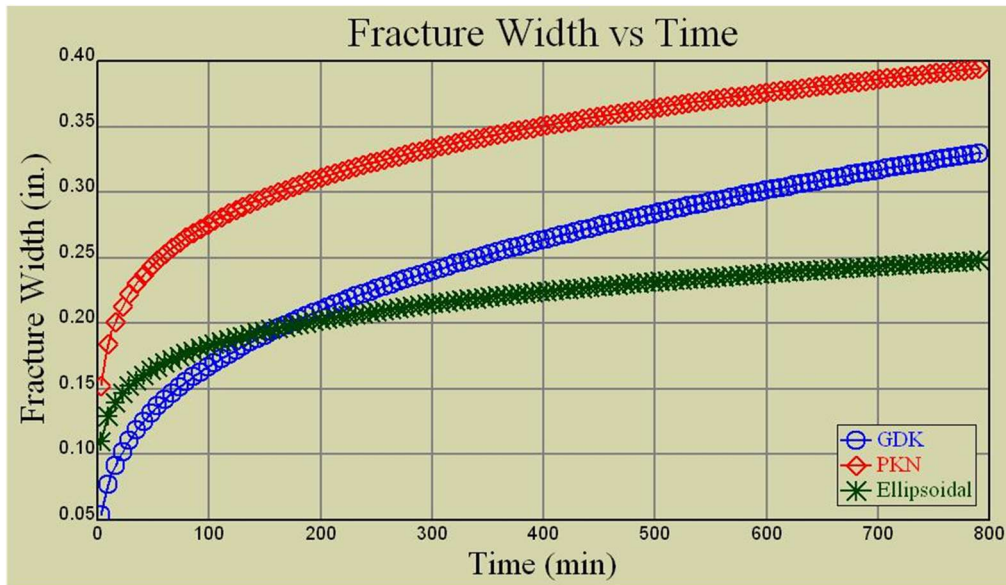**Figure 22: Variation of fracture width with fluid injection time in the Haynesville shale for q = 30 bpm. This figure was generated by MFAST (Meyer & Associates, 2009).**

Table 10: Influence of fluid injection rates and injection volumes on computed fracture geometry in the Haynesville shale

HAYNESVILLE SHALE						
	Q = 1 M gal, q = 30 bpm, Leakoff = 0.0015 ft/min0.5			Q = 400,000 gal, q = 30 bpm, Leakoff = 0.0015 ft/min$^{0.5}$		
Parameters	GDK	PKN	Ellipsoidal	GDK	PKN	Ellipsoidal
Length (ft) - 2L	934.65	932.35	1089.87	723.47	720.47	847.63
Height (ft)	934.70	932.00	1089.87	723.50	720.50	847.63
Max. Well Width (in.)	0.33	0.50	0.32	0.29	0.45	0.28
Ave. Well Width (in.)	0.33	0.39	0.25	0.29	0.35	0.22
Ave. Frac. Width (in.)	0.26	0.29	0.21	0.23	0.25	0.19
Net Pressure (psi)	39.92	47.91	52.99	46.07	55.38	61.08
Pumping Time (min)	793.65	793.65	793.65	317.46	317.46	317.46
	Q = 1 M gal, q = 120 bpm, Leakoff = 0.0015 ft/min$^{0.5}$			Q = 400,000 gal, q = 120 bpm, Leakoff = 0.0015 ft/min$^{0.5}$		
Parameters	GDK	PKN	Ellipsoidal	GDK	PKN	Ellipsoidal
Length (ft) - 2L	1182.03	1172.08	1402.61	887.00	876.27	1059.09
Height (ft)	1182.00	1172.20	1402.61	886.80	876.20	1059.09
Max. Well Width (in.)	0.47	0.71	0.45	0.41	0.63	0.40
Ave. Well Width (in.)	0.47	0.56	0.35	0.41	0.49	0.31
Ave. Frac. Width (in.)	0.37	0.40	0.30	0.32	0.36	0.27
Net Pressure (psi)	44.82	54.01	59.70	52.64	63.71	70.00
Pumping Time (min)	198.41	198.41	198.41	79.37	79.37	79.37

4. COMPARISON OF NUMERICAL RESULTS FOR SHALE BASINS

4.1 DEPTH TO FRACTURE (d_f)

In this section, depth to fracture for the four shale basins previously discussed are compared and the results are presented below. The clearance depth to groundwater table was investigated for fracture propagation in Barnett, Marcellus, Fayetteville, and Haynesville shale reservoirs. Circular fractures were assumed and depth to fracture was calculated as illustrated in Figure 23. The depth to fracture (d_f), which is the clearance depth in individual shale basins was evaluated based on the fluid injection volume of 400,000 gal and at different fluid injection rates of 30 bpm and 120 bpm. The leakoff coefficient was assumed to be 0.0015 ft/min$^{1/2}$, which is an appropriate value for intact shale and fairly conservative. The depth of each shale layer has a range as shown in Table 11. An average value in the reported range was selected as the injection depth (d_i) in the calculations. The depth of injection, d_i, was assumed to be at the middle of the payzone layer. The value of d_i was different for different shale layers as shown in Table 11 and Table 12.
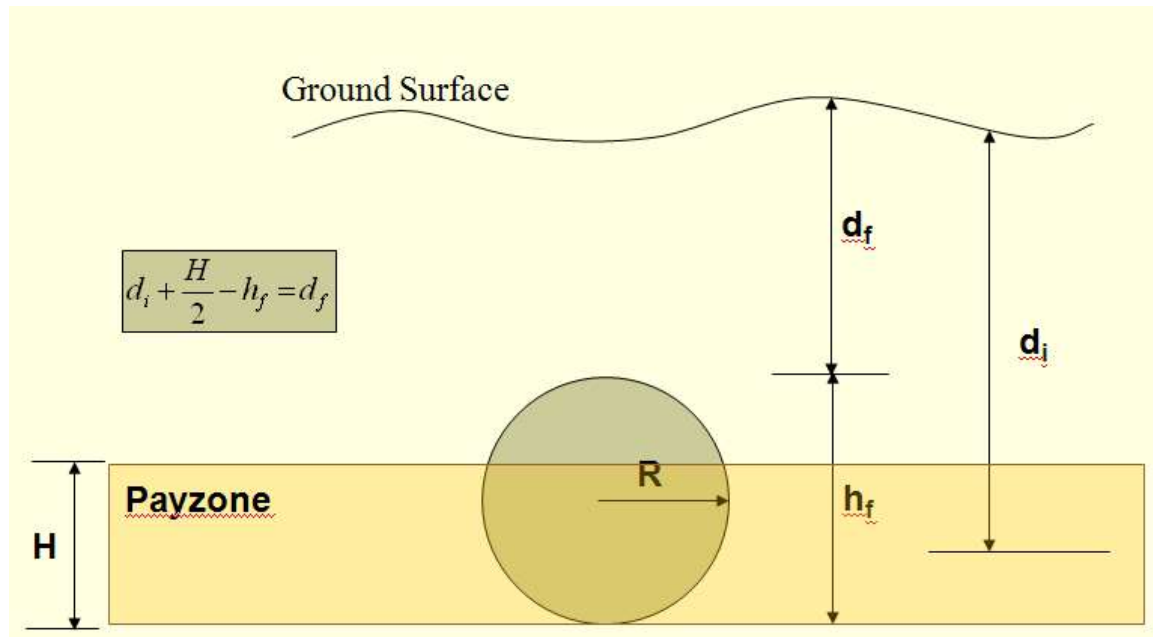
Figure 23: Schematic figure that defines the depth to fracture.

Figure 24 and Figure 25 show the comparisons of depth to fracture (d_f) for the Barnett, Marcellus, Fayetteville, and Haynesville shales at fluid injection rates of 30 bpm and 120 bpm. The amount of injection volume for each of these cases is 400,000 gal and the leakoff coefficient is 0.0015 ft/min$^{1/2}$. Because the Haynesville shale formation is so much deeper, results show that the depth to fracture is largest for the Haynesville shale in comparison to other shale formations (Marcellus, Fayetteville and Barnett).

Figure 24: Depth to top of maximum fracture propagation height.
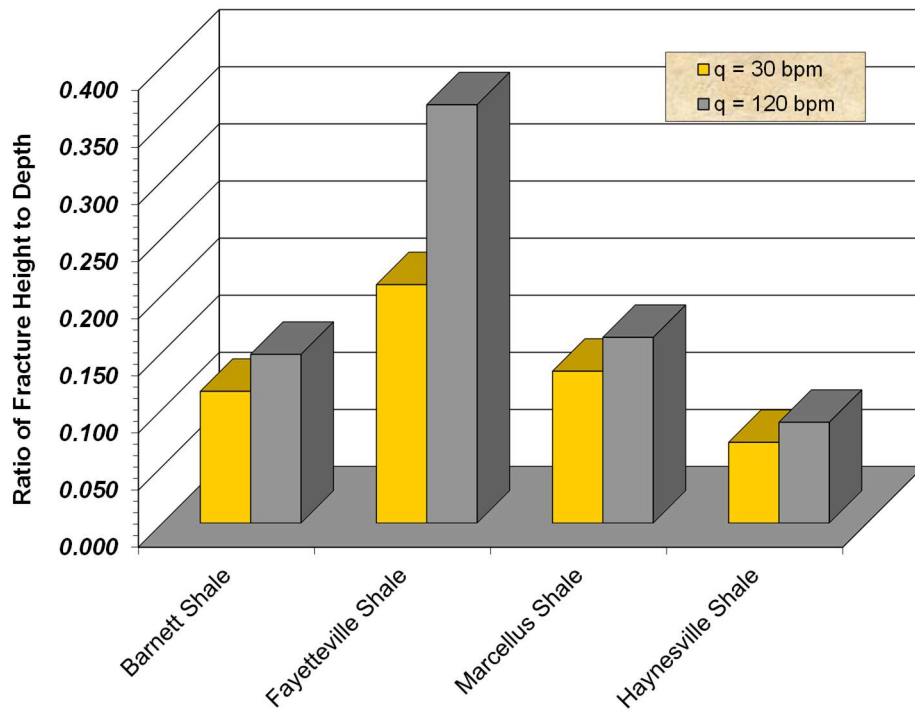
Figure 25: Ratio of fracture height to depth.

4.2   FRACTURE HEIGHT

Figure 26 shows the height of the penny-shaped fractures for the Barnett, Marcellus, Fayetteville, and Haynesville shales for fluid injection rates of 30 bpm and 120 bpm. The amount of injection volume for these cases was assumed to be 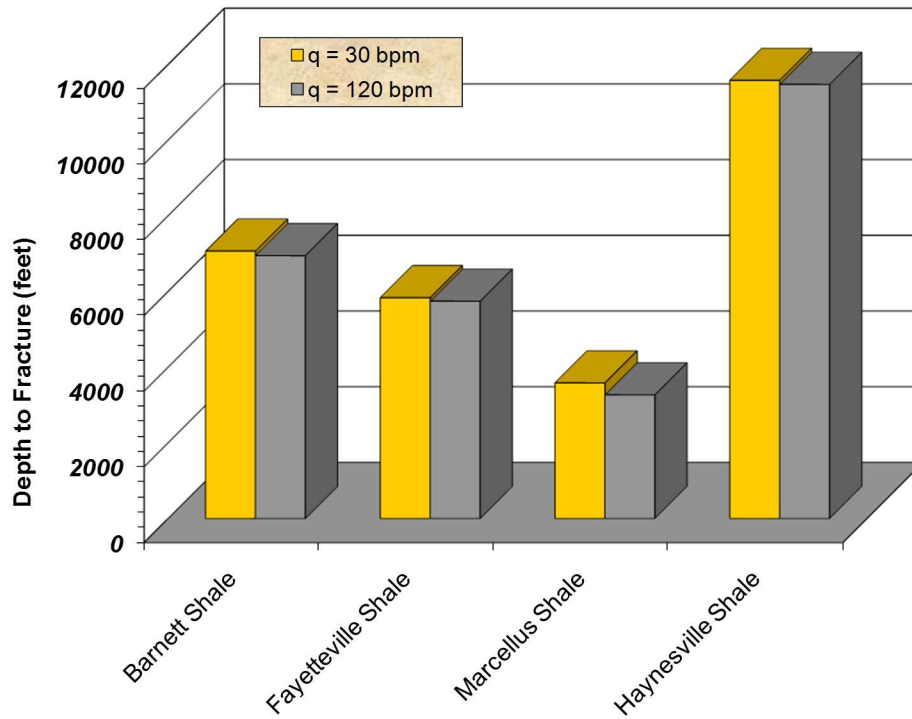400,000 gal. The leakoff coefficient used was 0.0015 ft/min$^{1/2}$. Results show that the computed value of fracture height is the largest for the Barnett shale at a fluid injection rate of 120 bpm. Also, the Ellipsoidal fracture model predicts the largest fracture height in general. The numerical values of payzone height, fracture height, and depth to fracture (d_f) for fluid injection rates of 30 bpm and 120 bpm for Barnett, Marcellus, Fayetteville and Haynesville shale reservoirs are presented in Tables 11 and 12 for the Ellipsoidal fracture model (aspect ratio = 1).
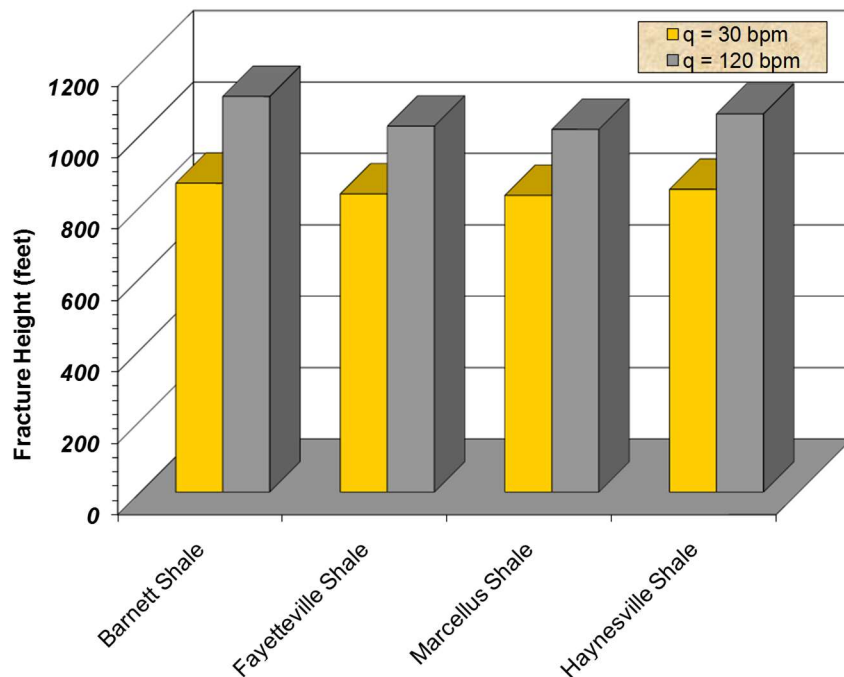
Figure 26: Computed fracture height for each shale in this study.

Table 11: Details of computed fracture geometry for q=30 bpm

Gas Shale Basin	Depth Range (ft)	Payzone Height (ft)	Average Depth (ft)	Average Payzone (ft)	Fracture Height (ft)	Top Depth to Fracture (ft)
Barnett	6,500–8,500	300–500	7,500	400	865	5,971
Marcellus	4,000–8,500	50–300	6,250	175	831	4,676
Fayettville	1,000–7,000	20–200	4,000	110	835	2,386
Haynesville	10,500–13,500	50–100	12,000	75	848	10,342

Table 12: Details of computed fracture geometry for q=120 bpm

Gas Shale Basin	Depth Range (ft)	Payzone Height (ft)	Average Depth (ft)	Average Payzone (ft)	Fracture Height (ft)	Top Depth to Fracture (ft)
Barnett	6,500–8,500	300–500	7,500	400	1,108	5,485
Marcellus	4,000–8,500	50–300	6,250	175	1,016	4,306
Fayettville	1,000–7,000	20–200	4,000	110	1,025	2,005
Haynesville	10,500–13,500	50–100	12,000	75	1,059	9,919

4.3 COMPUTED RESULTS ON CLEARANCE TO GROUNDWATER TABLE (d_f-d_w)

Figure 27 and Figure 28 show the clearance distance between the groundwater table and the top of the computed fracture for individual shale formations at fluid injection rates of 30 bpm and 120 bpm, respectively. The depth of groundwater table was assumed as shown in these figures. The amount of injection volume was assumed to be 400,000 gal and the leakoff coefficient used was assumed to be 0.0015 ft/min$^{1/2}$ for the calculations. Computations were performed using MFAST (Meyer & Associates, 2009). These figures show that Fayetteville shale formations have the lowest clearance depth among the four shale basins considered in this study. This clearance was calculated as 1,886 ft for an injection volume of 400,000 gal at an injection rate of 30 bpm. The clearance to the groundwater table was computed as 1,505 ft for an injection volume of 400,000 gal at an injection rate of 120 bpm. A comparison of Figure 27 and Figure 28 shows that the injection rate has a small impact when considering whether fractures propagate near the deepest ground water aquifer.
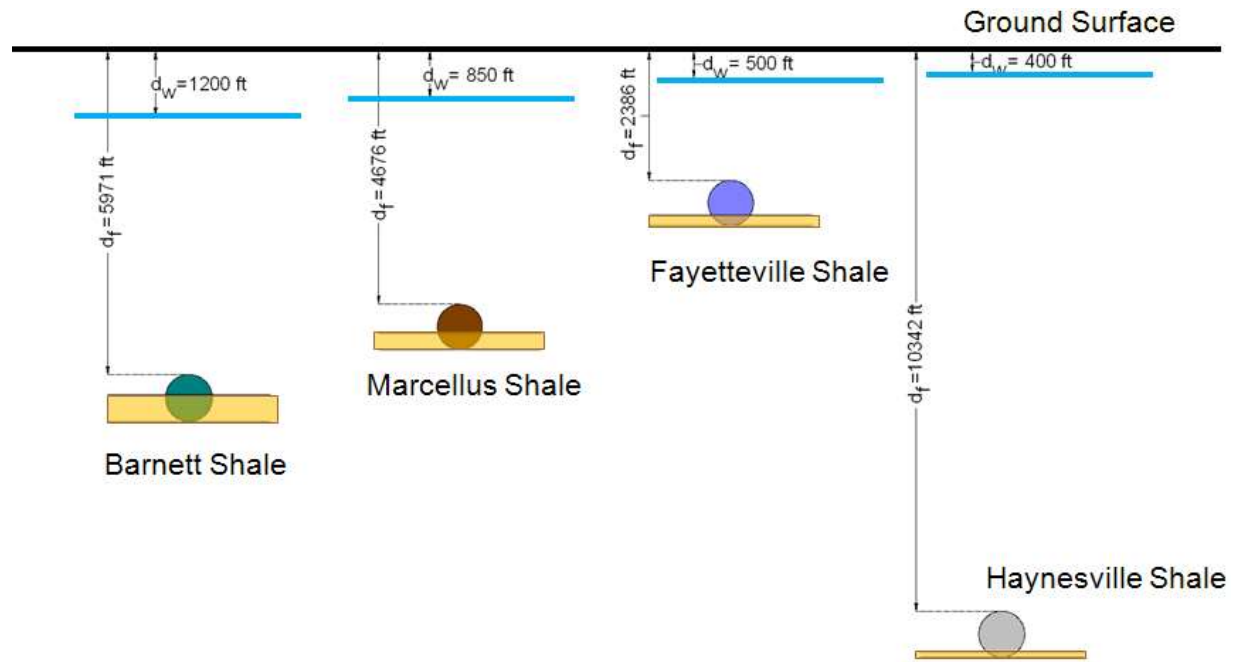

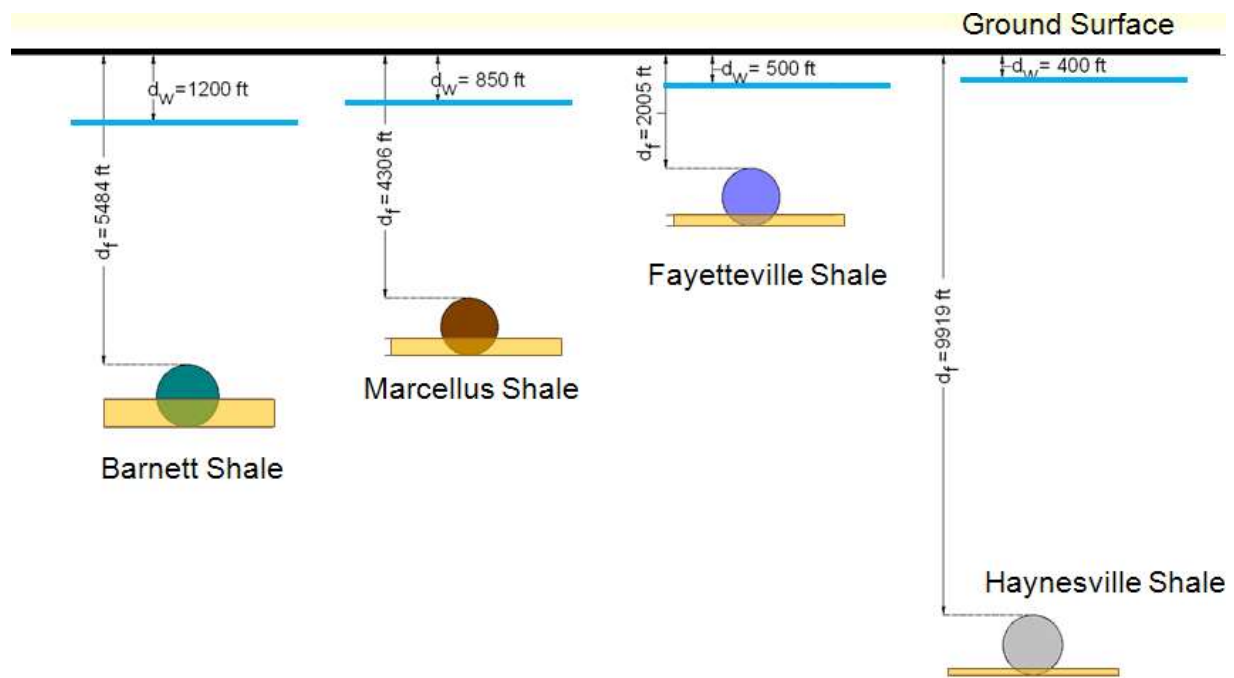**Figure 27: Depth to groundwater table and hydraulic fractures at q = 30 bpm.**

Figure 28: Depth to groundwater table and hydraulic fractures at q = 120 bpm.

5. <u>SUMMARY</u>

This study employs computer models of hydraulic fracture growth to assess the likelihood of hydraulic fractures extending upwards into shallow ground-water aquifers by calculating the height of hydraulic fracture growth in geologic formations above the pay zone during stimulation of gas shale reservoirs (Barnett shale, Marcellus shale, Fayetteville shale, and Haynesville shale). In these simulations, the vertical extent of the fracture was not restricted to the reservoir thickness. Instead, the fractures were allowed to propagate in the vertical direction without any constraints. A literature study was performed to evaluate properties such as gas contents, gas-in-place, depths, and depth to the base of groundwater table in these formations. Each shale formation was individually evaluated and compared with others.

In this study, the fracture length, fracture height, and fracture width were determined for different volumes of fluid injection and for different injection rates in shale reservoirs of Barnett, Marcellus, Fayetteville and Haynesville shales. The computations were performed based on three existing theories of fracture propagation (PKN, GDK and Ellipsoidal models). The study was based on the assumption of a hydraulic fracture that is initiated at the center of the shale layer during the process of hydraulic fracturing. Computations were performed using MFAST (Meyer & Associates, 2009). Results show an increase in fracture length and fracture width with an increase in the fluid injection volumes and fluid injection rates. Results also show that the fracture heights and depth to fractures varied significantly between these gas shale reservoirs. Furthermore, the results from this study show that the damage zone may not extend beyond 1,452 ft (Barnett Shale, Ellipsoidal model) for the assumed material properties used in the modeling study. Under assumed conditions, modeling results show that Barnett shale had the largest fracture height. Numerical results also show that Haynesville shale has the largest value of depth to fracture (d_f) and that Fayetteville shale formations have the smallest value of depth to fracture (d_f) among the four shale basins considered in this study.

6. REFERENCES

Arthur, J. D.; Bohm, B.; Layne, M. Hydraulic fracturing considerations for natural gas wells of the Marcellus shale. The Groundwater Protection Council, 2008 Annual Forum, Cincinnati, Ohio, Sept 21–24, 2008.

DOE and ALL Consulting. *Modern Shale Gas Development in the United States: A Primer;* U.S. Department of Energy Research, 2009.

Fisher, K.; Warpinski, N. Hydraulic Fracture-Height Growth: Real Data. SPE Annual Technical Conference and Exhibition*,* Denver, CO, 2011.

Gale, J. F. W.; Reed, R. M.; Holder, J. Natural fractures in the Barnett shale and their importance for hydraulic fracture treatments. *AAPG Bulletin* **2007,** *91*, 603–622.

Geertsma, J.; De Klerk, F. A rapid method of predicting width and extent of hydraulically induced fractures. *Journal of Petroleum Technology* **1969,** *21*, 1571–1581.

LaFollete, R. F.; Schein, G. *Understanding the Barnett shale, Oil and Gas Investor*; Hart Energy Publishing: Houston, TX, 2007.

Lecompte, B.; Franquet, J. A.; Jacobi, D.; Baker, H. Evaluation of Haynesville shale vertical well completions with a mineralogy based approach to reservoir geomechanics. Society of Petroleum Engineers, SPE Annual Technical Conference and Exhibition, New Orleans, LA, Oct 4–7, 2009.

Meyer, B. R. Design formulae for 2-D and 3-D vertical hydraulic fractures: Model comparison and parametric studies. Proceedings of the Unconventional Gas Technology Symposium of the Society of Petroleum Engineers, Louisville, KY, May 18–21, 1986; SPE paper 15240.

Meyer, B. R. Three-dimensional hydraulic fracturing simulation on personal computers: Theory and comparison studies. Proceedings of the Society of Petroleum Engineers (SPE) Eastern Regional Meeting, Morgantown, WV, Oct 24–27, 1989; SPE paper 19239.

Meyer, B. R.; Hagel, M. W. Simulated mini-frac analysis. *Journal of Canadian Petroleum Technology* **1989,** *28*, 63–73.

MFAST Manuals; Fracturing Software; Meyer and Associates, Inc., 2009.

Nordgren, R. P. Propagation of a vertical hydraulic fracture. *Society of Petroleum Engineers Journal* **1972,** *12*, 306–314.

Perkins, T. K.; Kern, L. R. Widths of hydraulic fractures. *Journal of Petroleum Technology* **1961,** *13,* 937–949.

U.S. DEPARTMENT OF **ENERGY**

NE = TL NATIONAL ENERGY TECHNOLOGY LABORATORY

Sean Plasynski
Executive Director
Technology Development & Integration
Center
National Energy Technology Laboratory
U.S. Department of Energy

Jared Ciferno
Associate Director
Oil and Gas
Technology Development & Integration
Center
National Energy Technology Laboratory
U.S. Department of Energy

Elena Melchert
Director
Division of Upstream Oil and Gas
Research
U.S. Department of Energy

Cynthia Powell
Executive Director
Research & Innovation Center
National Energy Technology Laboratory
U.S. Department of Energy

NETL Technical Report Series